Bachelor Thesis

Modelling and characterisation of a pressure sensor implemented in surface channel technology

Author:
Bas van Laerhoven

UNIVERSITY OF TWENTE.

May 3, 2019

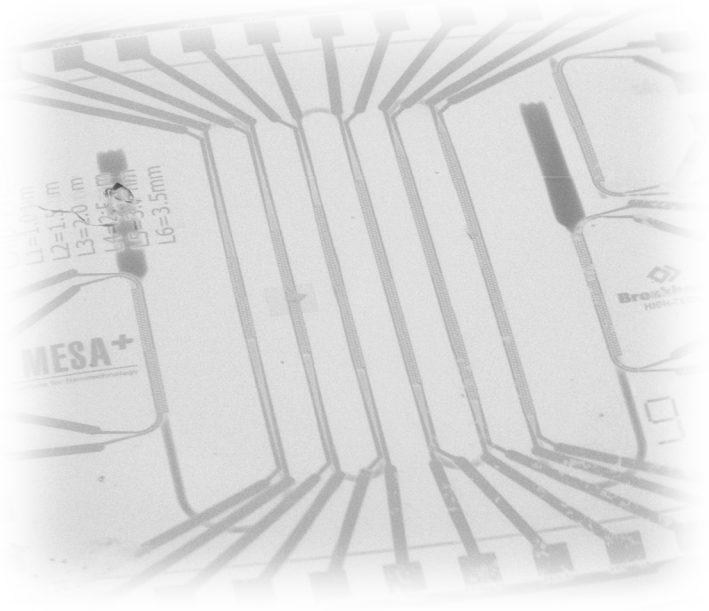

Bachelor Assignment Committee:
Dr.Ir.R.J.Wiegerink
Dr.Ir.J.Groenesteijn
Dr.Ir.M.Odijk
T.V.P.Schut MSc

1 Abstract

In several applications pressure sensors are being integrated in a chip in order to measure multiple parameters at the same time. To do this efficiently all the sensors need to be as efficient as possible, but also allow for an easy fabrication process where all the sensors can be combined into a single chip. To accomplish this, resistive pressure sensors are used that are made from metal strain gauges placed on top of a channel. Those strain gauges are positioned in Wheatstone configuration which allows a simple readout circuit.
For this research six pressure sensors, each with a different length, are compared with a theoretical model and with each other. The comparison includes dependence of length, influence of temperature, output sensitivity and influence of interference. The comparison can be made after creating a theoretical model and performing several types of measurements on the provided chips. From the comparison with the theoretical model it can be concluded that several assumptions used in the model need to be studied more so they can be improved. A short research was done in accurately determining the Young's Modulus, but this was not feasible within this research. The theoretical resistances were calculated from the chip design and compared to the measured resistances. The differences between the theoretical and measured resistances are caused in the fabrication process where the chips end up with slightly different dimensions as in the design.
From the comparison of the sensors with each other relations were found between the temperature, and the offset introduced by the readout circuit. Bigger fluctuations in temperature cause the offset of the signal to rise and deviate more. A relation was discovered between the initial offset from the measurement setup and the standard deviation of the output signals. This relation showed that a higher offset is accompanied with a bigger deviation. Measurements with a Faraday case showed that the standard deviation can be reduced, the temperature and interference from outside play an important role in this. All the results from the measurements are presented and discussed and from those results recommendations and improvements for future work are presented. The research shows promising results for the future because there are several points where the pressure sensors can be improved.

Contents

2 Introduction

2.1 Background

In current applications pressure sensors are being used to measure how much fluid or gas travels through a channel. If the pressure is combined with other parameters like mass flow, density and viscosity a lot of information about the fluid or gas can be obtained. Such applications can be used in several industries, for example to accurately determine the dosage of medicine. Currently pressure sensors are integrated in sensors like the Coriolis mass flow sensor, on which extensive research has already been done. In the earliest versions these pressure sensors were capacitive, which had several disadvantages such as low sensitivity, large drift and crosstalk with other capacitive sensors [1]. Therefore the switch was made to resistive pressure sensors. The resistive pressure sensor uses a Wheatstone configuration and does not need complex readout electronics. These sensors not only made the fabrication process easier but also increased sensitivity, lowered the drift and allowed a simultaneous operation with other sensors [2].

2.2 Aim of the research

The aim of this research is to get better knowledge about the underlying physics of the resistive pressure sensors used for multiparameter measurements. In this research a theoretical model is created which explains the behaviour of these pressure sensors. This model discusses concepts like the deflection and strain of a channel created with surface channel technology. On top of this channel metal strain gauges are patterned in a Wheatstone configuration. The combination of those concepts leads to a sensor output which is based on: material properties, dimensions of the sensors, supply voltage and the applied pressure. The theoretical model will be compared with measurements performed on chips provided by Bronkorst High-Tech BV. By looking at the influences of temperature, offset and interference; characteristics of the pressure sensors can be determined. The results from the measurements will be compared with the theoretical model to see how these characteristics influence the working principle of the sensors. By understanding how the temperature, offset and interference influence the performance of the pressure sensors, solutions can be found in which the already existing pressure sensors can be improved to make them more accurate and usable in combinations with other sensors.

2.3 Outline

In chapter 2 the theoretical concepts of a resistive pressure sensor are explained. The different concepts of deflection, strain, the principle working of a strain gauge and readout of a Wheatstone bridge combine into a theoretical model that describes the output of the pressure sensor which is dependent on dimensions, material properties, pressure and applied voltage.
The measurement setup used in this research is explained in chapter 3. The way in which this setup operates is important to understand how the applied voltage and interference work on the signals. Next to that the several measurements that are performed are explained which results in four research questions that need to be answered at the end of the research.
In chapter 4 the results from the measurements are discussed together with a more in-depth analysis of these results. Based on observations more research was performed in specific parts of the measurements like the dependence of temperature and the source of interference.
Chapter 5 reflects on the results and in this chapter the research questions set in chapter 3 are answered. Some results do not give clear answers and are therefore accompanied with a discussion. This chapter is concluded with recommendations and improvements for future research.

3 Theory

In this chapter fundamental knowledge is provided to understand how a pressure sensor is made and how it operates. This chapter is used as the basis on which the following chapters will continue.

3.1 Surface channel technology

Surface channel technology (SCT) allows the industry to continue the downscaling of MEMS fluidic devices. The technology makes it possible to place structures close to the fluidic channel, which is convenient for all kinds of purposes. For example, structures to measure the deformation of the channel roof [3]. Surface microchannels are created using a one-mask process scheme, such a scheme is visible in Figure 1a. This scheme consists of three steps. First, the etch holes which are 2 μm in width and 5 μm in length are combined into segmented lines. Each line eventually becomes a microchannel. This mask layout is placed onto a silicon-rich silicon nitride (SiRN) layer low pressure chemical vapour deposition (LPCVD) [4] (Figure 1a (a)). In the second step, the channels are etched through the etch holes. Neighbouring etch surfaces are combined, resulting in semicircular long channels (Figure 1a(b)). In the third step the etch holes are closed with a SiRN layer, this layer also uniformly covers the inside of the microchannel (Figure 1a(c)) [5]. The result of this process is a sealed semi-circular microchannel. In the case of this research this microchannel has a flat ceiling which is approximately 91μm wide and 3.5μm high. The fact that the ceiling is flat is important for the remainder of the research.

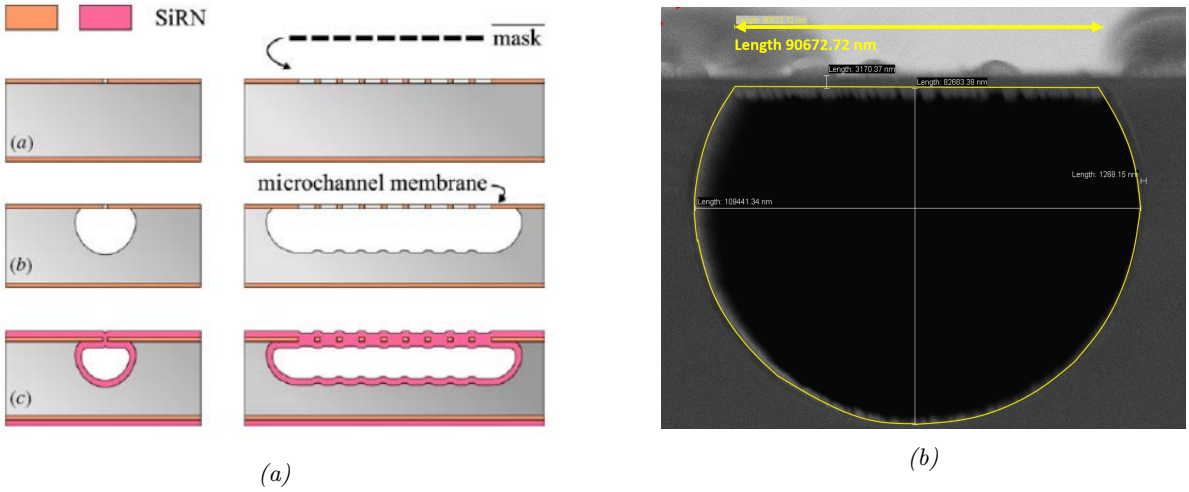

(a) *(b)*

Figure 1: (a) Surface microchannel process scheme. Figure taken from [5]. (b) a SEM photograph of the microchannel.

3.2 Chip layout

For this research several chips were provided, the chips were fabricated on two different wafers but the design is identical for each chip. Every chip consists of nine pressure sensors. The sensors and their lengths are visible in Table 1. The way the sensors are named corresponds with Figure 2a.

Table 1: Names of the pressure sensors and their corresponding lengths. The length is defined as the part of the sensor which forms the Wheatstone configuration.

Sensor	length [mm]
Input	1.5
Sensor 1	1.0
Sensor 2	1.5
Sensor 3	2.0
Sensor 4	2.5
Sensor 5	3.0
Sensor 6	3.5
Output	1.5
Reference	1.5

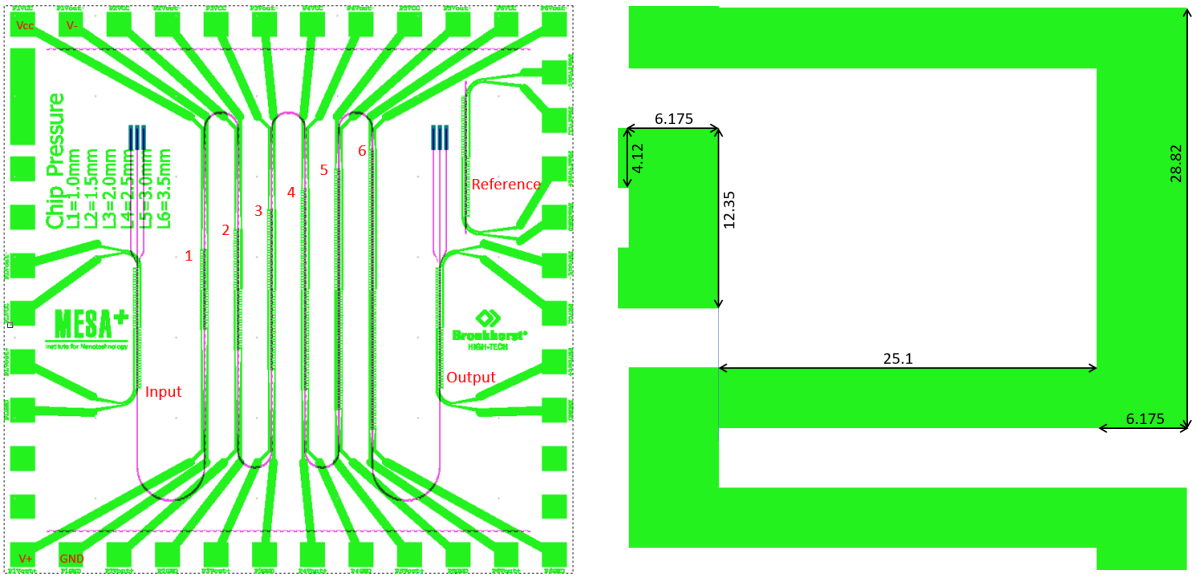

(a) *(b)*

Figure 2: (a) Chip design where all the sensors are labelled with their corresponding names. (b) Dimensions of a single strain gauge and the connection parts, taken from the chip design. All dimensions are in µm.

All sensors, except the reference sensor, are placed on top of a microchannel through which a gas or fluid can flow. From the chip design the exact dimensions from the resistors and strain gauges can be found. Those dimensions are necessary to calculate the resistances of the sensors. In Figure 2b the most important dimensions are visible.

3.3 Deflection theory

As discussed in section 3.1 the microchannel has a flat ceiling. Because of the flat ceiling the approximation can be made that the ceiling is a fixed beam with a certain length width and height. The dimensions of the ceiling are already known from the previous sections. With this information a model can be made for the deformation of the ceiling of the microchannel. A second assumption that is made is that the substrate fixes the ceiling at both ends. With this assumption the behaviour of the ceiling can be described by equation 1 [6]. Where w is the deflection $[m]$, F is the applied pressure $[N/m^2]$, L is the length of the ceiling $[m]$, x is the position along the length $[m]$, E is the Young's Modulus and I is the second moment of area which is described by equation 2. The second moment of area uses the height (h) and width (b) of the beam $[m]$. It is important to notice that the length of the ceiling is the width of the channel from Figure 1b.

$$w = \frac{Fb}{24EI}x^2(L-x)^2 \quad (1) \qquad I = \frac{bh^3}{12} \quad (2)$$

Combining equation 1 & 2 leads to the expression described by equation 3.

$$w = \frac{F}{2Eh^3}x^2(L-x)^2 \quad (3)$$

With this expression the deflection at any point along the length of the beam can be calculated. Next to that, the pressure can be increased or decreased too see how the beam behaves. From the expression for the deflection an expression of the strain (relative elongation) that is exercised on the beam can be derived. This is done with the relation in equation 4. This relation is important for understanding the fundamentals of a strain gauge.

$$\varepsilon = \frac{h}{2}\frac{\partial^2 w}{\partial x^2} = \frac{F}{2Eh^2}(L^2 - 6x(L-x)) \quad (4)$$

Using this for a strain gauge the strain must be averaged over the length of the strain gauge. The result of this gives the average strain which is measured by a strain gauge. Using an estimate for the Young's Modulus of 210 GPa, a pressure varying from 0 to 6 Bar Gauge pressure and dimensions taken from the chip layout; a visualisation can be made of how the channel will deform under pressure. This is visible in Figure 3a. For the strain a similar visualisation can be made. This is visible in Figure 3b. What is noticeable from the visualisation of the strain is that there are points where the strain is not measured. Those are the positions in the chip layout where the connection parts are located which connect the individual strain gauges. Another thing is that there are two points where the strain is zero. Ideally those two points should be located at the points where the strain is not measured. This would mean a change in chip design where not every strain gauge would have the same length.

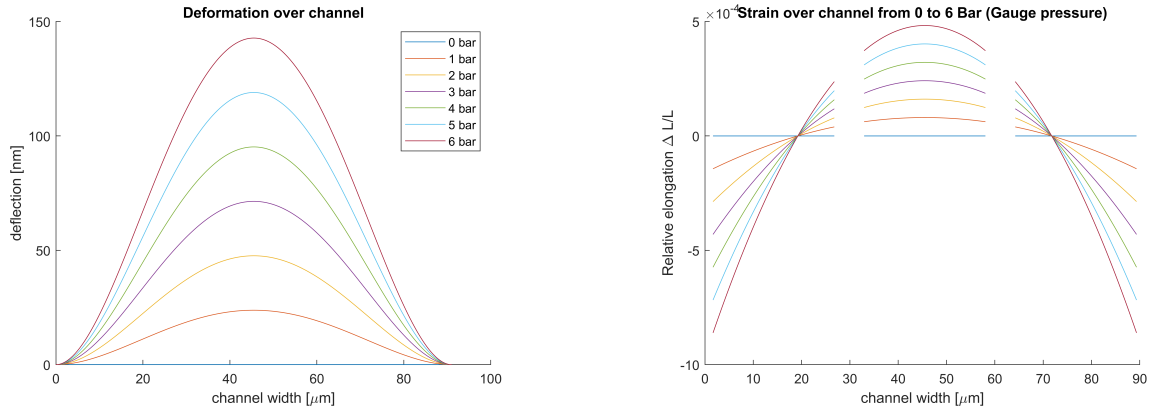

(a) *(b)*

Figure 3: (a) Visualisation of the theoretical deflection of the channel under a pressure varying from 0-6 Bar (Gauge pressure). (b) Visualisation of the theoretical strain exercised on the strain gauges. The pressure is varied from 0-6 Bar (Gauge pressure). Legend from figure (a) applies for both figures. (MATLAB script used to generate figures visible in Appendix D.)

3.4 Young's Modulus

Looking at equation 4, the Young's Modulus is an important material property. To be able to calculate the strain the Young's Modulus should be as accurate as possible. The Young's Modulus is defined as the ratio between stress and strain. Strain is the relative elongation of a material, stress is the force (F) per unit area of a material (A). In expressions this translates to Equations 5 & 6.

$$strain(\varepsilon) = \frac{\Delta L}{L} \tag{5}$$

$$stress(\sigma) = \frac{F}{A} \tag{6}$$

This combines to the ratio which defines the Young's modulus as is visible in equation 7.

$$E = \frac{\varepsilon}{\sigma} \tag{7}$$

3.5 Principle working of the strain gauge

The strain gauge is a sensor which translates force, pressure, tension and other forces into a change in electrical resistance. This makes the strain gauge a good candidate to be used as a pressure sensor. In this research a pressure sensor is made up from four resistors, placed in a Wheatstone configuration on top of the microchannel. Each resistor is made up from gold strain gauges that are placed perpendicular to the direction of the channel. This configuration is visible in figure 4, when a pressure is applied the strain gauges in the middle are elongated while the strain gauges at the sides are compressed. This will respectively result in a positive and negative strain in the strain gauges. It can be assumed that the strain gauge follows the behaviour of the channel ceiling and that it does not influence the movement of the ceiling. This is because the Young's Modulus of gold is in the range of 80 GPa where the Young's Modulus of SiRN is in the range of 210 GPa [7], making the gold much more elastic. Because of this equation 4 can be used to calculate the elongation of each strain gauge. The electrical resistance of a strain gauge is defined by equation 8, where ρ is the resistivity of the material [Ωm], l is the length of the strain gauge [m] and A is the cross-sectional area of the strain gauge [m^2].

$$R = \rho \frac{l}{A} \tag{8}$$

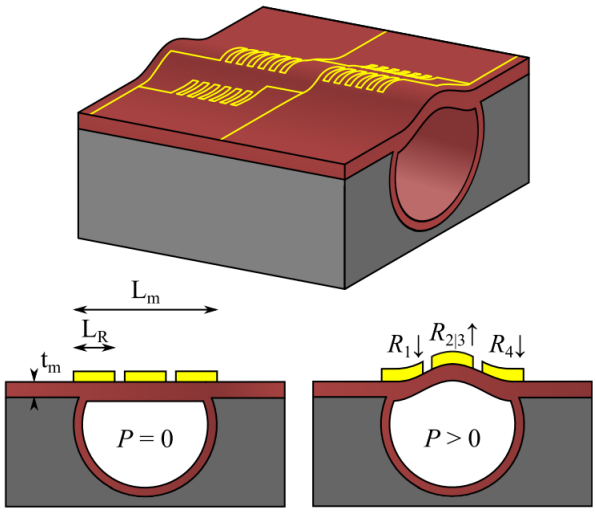

Figure 4: Design of a resistive pressure sensor. Gold strain gauges are placed on top of the channel roof. When under pressure the strain gauges are elongated or compressed changing their resistance. Figure taken from [2].

3.6 Readout of pressure sensors

As mentioned in the previous section, a pressure sensor is made from four resistors placed in a Wheatstone configuration. All four resistors are equal in length, giving them the same resistance at atmospheric pressure. The output voltage (V_{out}) of the Wheatstone bridge is given by equation 9. Figure 5 shows the circuit diagram where the same configuration as in Figure 4 is used. In this configuration resistors R_1 & R_4 are compressed and resistors R_2 & R_3 are elongated. Because of the symmetry the resistances can be expressed as a rest resistance (R_w) with a change in resistance (ΔR), this results in equation 10. In this situation the rest resistance (R_w) is the resistance of the Wheatstone bridge in rest position, where the gauge pressure is 0 Bar. The resistance of wires that are connected to this Wheatstone bridge are not included yet.

$$V_{out} = V_{in}\left(\frac{R_2}{R_1+R_2} - \frac{R_4}{R_3+R_4}\right) \tag{9}$$

$$\begin{aligned} R_1 &= R_4 = R_w - \Delta R_{1,4} \\ R_2 &= R_3 = R_w + \Delta R_{2,3} \end{aligned} \tag{10}$$

The expressions from equation 10 can be substituted in equation 9:

$$\begin{aligned} V_{out} &= V_{in}\left(\frac{R_w + \Delta R_{2,3}}{2R_w + \Delta R_{2,3} - \Delta R_{1,4}} - \frac{R_w - \Delta R_{1,4}}{2R_w + \Delta R_{2,3} - \Delta R_{1,4}}\right) \\ &= V_{in}\left(\frac{\Delta R_{2,3} + \Delta R_{1,4}}{2R_w + \Delta R_{2,3} - \Delta R_{1,4}}\right) \end{aligned} \tag{11}$$

The initial resistance (R_w) is in the range of 100-400 Ω, depending on the length of the sensor. The change in resistance of the resistors (ΔR) will be in the order of milliohms. Therefore, it is safe to make the assumption that $2R_w >> \Delta R_{2,3} - \Delta R_{1,4}$. Because of this assumption V_{out} can be simplified to equation 12.

$$V_{out} = V_{in}\left(\frac{\Delta R_{2,3} + \Delta R_{1,4}}{2R_w}\right) \tag{12}$$

The expression for V_{out} from equation 12 shows that V_{out} is linearly proportional to the change in resistance. Later on it will be discussed if the change in resistance is linearly proportional to the applied pressure, which would be the ideal case. The connections from the voltage supply to the Wheatstone bridge are neglected up until now. In a realistic situation the connecting wires can not be neglected. To compensate for this, V_{in} can be represented as a function of a voltage divider. This is visible in equation 13. In this equation R_s and R_g represent the resistances of respectively the input and output connections, because those connections are equal in length they can be substituted.

$$V_{in} = \frac{R_w}{R_s + R_w + R_g}V_{cc} = \frac{R_w}{2R_s + R_w}V_{cc} \tag{13}$$

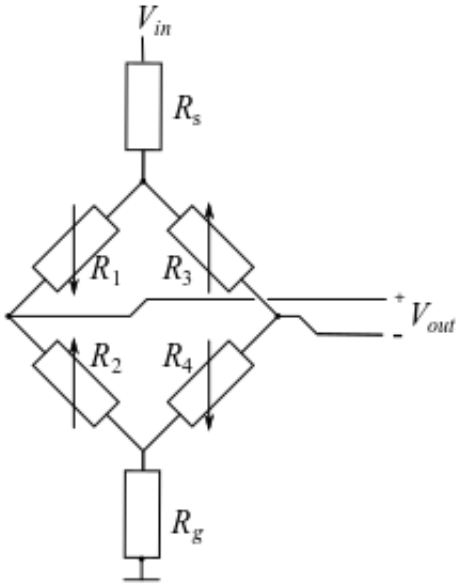

Figure 5: Circuit diagram representing the Wheatstone bridge. Resistances correspond with Figure 4. Figure adapted from [8].

Equation 12 gives the output voltage of the Wheatstone bridge. However, the output is dependent on the change in resistance, which is in the order of milliohms. Unless a large input voltage is used the output voltage will therefore also be very small. Applying a large input voltage is not desirable because a lot of heat will be dissipated in the resistors which could also influences the channel underneath. To prevent this a small voltage is used. The downside of this is that the output voltages need to be amplified in order to get measurable results. How the signal is exactly amplified will be discussed in the next chapter when the measurement setup is explained.

3.7 Combination to model

In the previous sections expressions for the strain, relations for the resistance of a strain gauge and an expression for the output voltage depending on the changing resistance were discussed. Those expressions can be combined to see if the change in resistance is linearly proportional to the change in pressure. For a metal strain gauge the relative change in resistance is dominated by the change of geometry. Because of that the piezoresistive effect can be neglected. In other types of strain gauges the change of resistivity due to deformation is larger which requires an extra part to the expression. From the expression in equation 14, where ν is the Poisson ratio which is typically 25%, we see that the relative change in resistance is proportional to the strain. This expression is called the gauge factor (G)[9].

$$\frac{\Delta R}{R_w} = (1 + 2\nu)\varepsilon \tag{14}$$

Equation 14 shows that the relative change in resistance is equal to the strain multiplied with a constant. As already explained in section 3.6 the output voltage is linearly proportional to the change in resistance. So the output voltage is linearly proportional to the strain. Looking back to equation 4, the strain is dependent on the applied pressure. Combining all this knowledge leads to the conclusion that the output voltage of the sensors is linearly proportional to the pressure. Equation 14 can be substituted into equation 12, this gives the expression visible in equation 15.

$$V_{out} = V_{in}\left(\frac{\varepsilon_{2,3} + \varepsilon_{1,4}}{2R_w}\right) R_w(1 + 2\nu) \tag{15}$$

In order for the output voltage to be correct the resistances of all the sensors need to be calculated. This is done with the help of Figures 2a, 2b and equation 8. From the figures all the separate components of each sensor can be identified, with the equation the theoretical resistance of each component can be calculated. This is done

with the model from Appendix A This leads to the resistance values visible in Table 2. The resistances are calculated from the voltage supply to ground, using all four resistors in the Wheatstone bridge. The connecting arms to V_- and V_+ are not taken into consideration.

Table 2: Theoretic resistances of all the sensors. Calculated with the dimensions from the chip layout from Figure 2b.

Resistances	Resistances of the sensors in Ohm [Ω]								
	Sensor 1	Sensor 2	Sensor 3	Sensor 4	Sensor 5	Sensor 6	Input	Output	Reference
R without connections	157.77	241.91	315.54	399.68	483.82	567.97	241.91	241.91	241.94
R connections	21.99	17.69	14.02	8.06	5.47	2.87	6.35	6.35	8.13
R total	179.75	259.60	329.55	407.74	489.29	570.84	248.26	248.26	250.04

In the next chapters it will become clear if the chips that are measured behave as can be expected from the theory discussed in this chapter and if indeed the output of the sensors changes linearly with the pressure. Also, from equation 15 it can be concluded that the output of the sensor is dependent on the input voltage and the strain. And is independent from the rest resistance (R_w). This means that only looking at the Wheatstone configurations all the sensors should have the same output. In reality this will most likely not be the case because almost every sensor has a different length of connecting wires which influence the input voltage. Next to that, in the longer sensors it can occur that there is a pressured drop which results in a lower average strain.

4 Measurements

This chapter explains of which components the measurement setup consists and how all those components are combined to form one functioning setup. Next to that it is explained which measurements are performed with the setup.

4.1 Setup

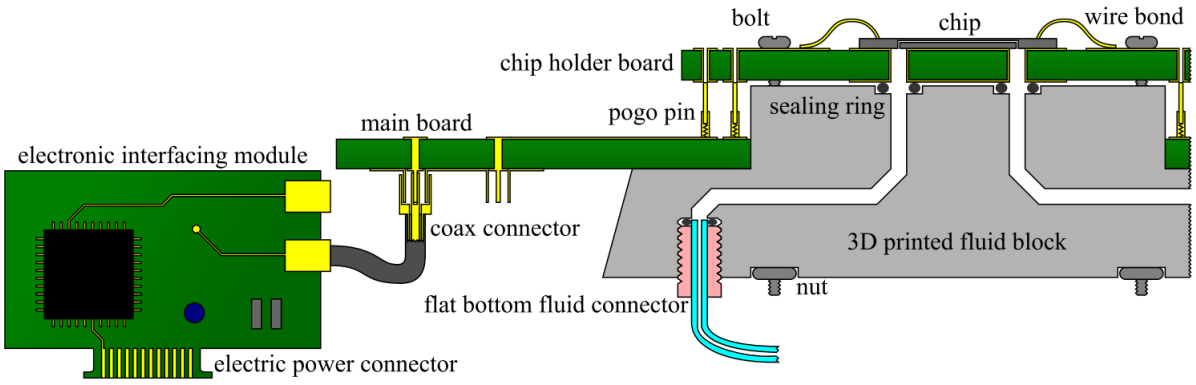

Figure 6: All components of the interfacing platform. The chip is mounted on a chipboard, this board is electrically connected to a main board via pogo pins. The chipboard is fluidically connected with a 3D printed fluid block. The main board is connected to the modules with Coax cables. Figure taken from [10].

The measurement setup consists of several parts. Figure 6 shows how this looks in a schematic. A complete picture of how the total measurement setup looks is visible in Figure 8. Setting up this measurement setup consists of several steps. First, the chips are glued to a chipboard. The bond pads on the chip are connected to the chipboard with wire bonds. The chipboard also has six fluid/gas connections below the chip those will be used later to allow a gas/liquid to flow through the chip.
The chipboard connects to a mainboard via connection with pogopins. This mainboard connects the chipboards to the the fluid/gas and to the measurement equipment. Each connector on the mainboard is connected to a specified connection on the chip. The exact specification of how the connections are assigned is visible in Appendix B. The connectors on the mainboard are connected to five modules, which are the AC Wheatstone bridge readouts, through COAX cables. Each readout module is connected to two sensors. The AC Wheatstone bridge readout uses a square wave (AC signal) at a frequency of 1 kHz, with an amplitude of 130 mV.
The two output voltages that are measured from the Wheatstone bridge are amplified by an instrumentation amplifier. After amplification the signal can be demodulated and an offset is subtracted using a digital-to-analog converter (DAC). After demodulation the signal is low-pass filtered, amplified again and connected to an analog-to-digital converter (ADC). This process is visible in Figure 7. All the AC bridge readouts have their own address which is set using switches on the readout modules, in this way all the sensors can be readout separately. Next to the five readout modules two ADC modules are used to convert all the readouts back to digital signals and send them to the computer.

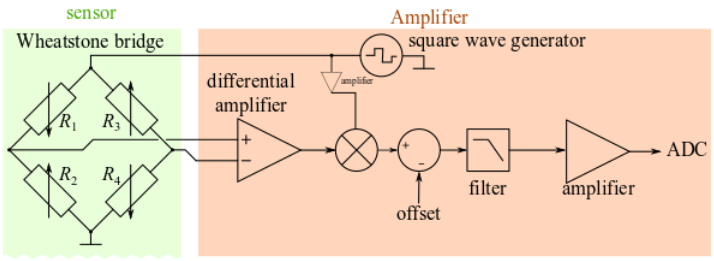

Figure 7: Schematic overview of how the readout modules process the output voltages from the Wheatstone bridge. Figure adapted from [11].

On the other side of the measurement setup the 3D printed fluid block allows for eight fluidic/gas connections, for this measurement only two of those connections are used, one input and one output. The gas used in the measurements is nitrogen. The nitrogen is supplied to a pressure controller at a pressure of eight bar absolute pressure. The pressure controller can increase/decrease the pressure in steps, and hold them for a specific time step. Those steps can be chosen and varied for different measurements in a Python script.
After the pressure controller there is a flow meter which checks the incoming flow and sends the data to the computer. After the flow meter the nitrogen enters the mainboard and goes through the entire chip. When the nitrogen exits the chip it encounters a second flow meter which checks the outgoing flow, by doing this pressure drops and leaks can be identified. After the flow meter the channel is blocked, the only way the nitrogen can leave the channel is via a small leakage valve which is placed between the pressure controller and first flow meter. The last part of the measurement setup is a temperature sensor which is located next to the mainboard, it would be more ideal to measure the temperature on the chip itself but this would complicate the measurement setup.
All the electronic equipment is supplied with a voltage of 6.2 V provided from a voltage supply. All the signals from the electronic equipment are send to a computer where they are processed using a code written in Python. The code generates a plot where data can be visualised, also all the data is being saved so it can be processed at a later time. The save file of the data contains the following important parameters: Time, FlowIn, FlowOut, Pressure, Pressure (set point), Temperature, Pressure In, P1, P2, P3, P4, P5, P6, Pressure Out and Pressure Reference.

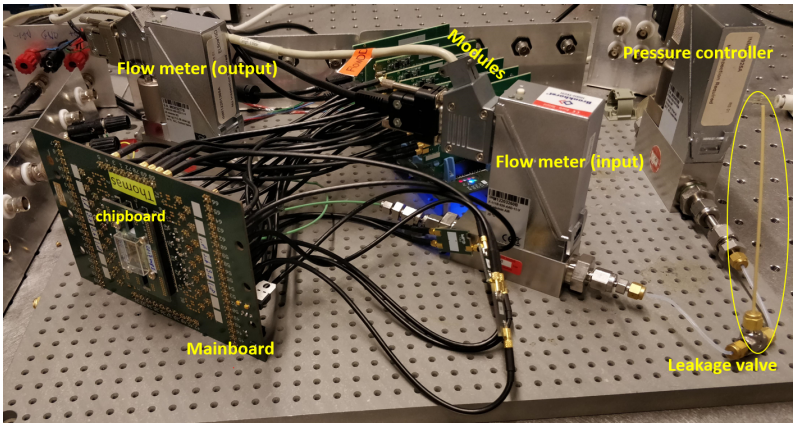

Figure 8: Picture of the complete measurement setup. Key aspects are labelled with their corresponding names.

4.2 Output of the measurement

The data obtained from the measurement needs to be analysed, this is done using MATLAB (Version R2018b), the exact script is visible in Appendix E. The data from Pressure In up until Pressure Out is easily plotted against the time. The output from the sensors is in Volt (V), when comparing the results of the measurement to the theoretical model the amplification introduced by the measurement equipment must be taken into account. Due to the several amplification steps explained above the signal is amplified a total of 38,649×. Next to that, every sensor has a different offset and starts at a slightly different point, this complicates the process of comparing the sensors because they do not start at the same point. In order to compensate for this every signal is subtracted with the average of the minimum value. After the subtraction all the sensors will have approximately zero as their minimum value making it easier to compare the results.

In order to make sure that the results from the measurements are reliable several parameters need to be set. If the parameters are different for every measurement the results are harder to compare. The pressure is increased in a specified amount of steps, for the measurements it is chosen to vary the pressure from 1.2 to 7 Bar absolute pressure. This is done in 15 steps, after that the pressure is reduced again until 1.2 Bar. In total this cycle takes 30 pressure steps. To ensure that the channel has time to adjust to the pressure each step is held for 300 seconds. Especially in the second half of the cycle it is important to have enough time for each step because the excessive pressure needs to flow away through the small leakage valve. In total one cycle takes up five hours. To look at the consistency of the chips it is preferred to perform at least two measurement cycles.

4.3 Young's Modulus

When calculating the strain the Young's Modulus (E) is an important material property. To make a theoretical model the Young's Modulus should be as close to reality as possible. To obtain this measurements are done with laser Doppler vibrometry to look at the elongation of the material. The vibrometer shines a laser beam on the top of the chip, the reflected beam is compared with a reference beam. From this the intensity of the beam can be calculated. The difference in intensity can be translated to the height of the chip [7]. For this measurement a different sensor is used which consists of several circular channels with metal fingers on top. If the channel is put under pressure the metal fingers will deform, this deformation is measured by the vibrometer and from this the elongation can be determined. The measurement consists of several steps. First, a chip is placed under the microscope and must be levelled horizontally for the best result. Next the area of interest must be set by letting the equipment sweep over a large range and define the correct starting and end point. After that a measurement is done where the microscope sweeps over the defined area of interest. Results are obtained by multiple lines over the structure. The results give the height of the structure along this measurement line. After that post-measurement analysis can be done such as linear regression to make the substrate in the background a flat surface. The results can be averaged or filtered depending on how smooth the results look.

Research question:
Can the elongation of the structure be measured accurately to determine the Young's Modulus of the material?

4.4 Resistances

In Section 3.7 the theoretical resistances for the sensors are calculated. These resistances include the Wheatstone configurations and the connections from the voltage supply and ground to the sensor. Those theoretical resistances can be compared to measurements to check if the chips have the same characteristics as in theory. In order to measure this the chips are measured on the chipboards, this is the closest position to the chip where a measurement can be done. All the chips are measured from Voltage supply to ground, in this way the resistances of all four of the resistors in the Wheatstone configuration are measured.

Research question:
Are the measured resistances comparable to the theoretic resistances? If not, how can it be explained that the resistances are different from the theory?

4.5 Dependence of length

An important part of observing the results is looking for a relation between the output and the change in length. Looking back to Section 3.6, an expression is given for the output of the sensors (Equation 12). This expression is based on the initial resistance and the strain of the strain gauges. This expression is independent of the amount of strain gauges, in theory every strain gauge should give the same result. If all the sensors behave according to the theory the output for every sensor will be the same and the length will not be distinguishable. However, the connecting wires are different for every sensor, this gives every sensor a different resistance which is not solely dependent on the Wheatstone.

Research question:
Is there a distinguishable result between the output of the sensors? If so, can this result be explained by the contribution of the connecting wires?

4.6 Influence of noise

Because all nine sensors are being measured at the same time a lot of wires need to be connected at the same time, to be precise it requires 36 connections to monitor all nine of the sensors. Next to that the AC Wheatstone readout modules use a lot of amplification in order to get a measurable result. Besides that there are several more options that can influence the output signal. To be able to identify which aspects influence the signal several things can be done.
First, the sensors can be measured separately. For reference the input and output sensors will stay connected, next to that only one of the six sensors will be connected to a voltage supply. Repeating this for all six the sensors can give results if the sensors influence each other when they are all connected. The so far unused parameters, temperature, FlowIn and FlowOut can also be used to look at influences, if there are disturbances in the output signal they are compared with the temperature and flow to see if the disturbances are caused by changes in the temperature or flow. The sensor output can be filtered to see if changes in temperature result in more or less noise in the output.

Research question:
Can the source of the noise be identified? If so, in what ways can the noise be minimised?

5 Results

In this chapter results from the measurements are presented. These results correspond to the measurements discussed in the previous chapter. The results are analysed to see if the research questions set in the previous chapter can be answered.

5.1 Young's Modulus

The method described in section 4.3 is used to determine the Young's Modulus of SiRN. First the results from the measurement vibrometer are discussed. The first sensor is placed under the microscope so the desired area can be found. As is explained the substrate around the sensor is linearised so it is considered a flat surface. After this the measurement lines placed over the structure give the height along the line. This measurement was repeated five times, every time the pressure was increased with 1 bar. The results of these measurements are visible in Figure 9. Those results can be compared with each other to see if the roof rises when the pressure is increased. The results of those differences are visible in Figure 10.

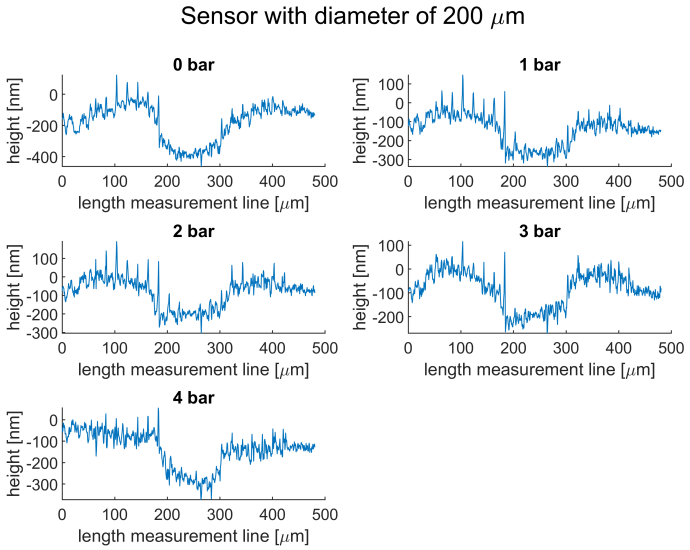

Figure 9: Results for the height along the measurement line for a varying pressure from 0-4 bar.

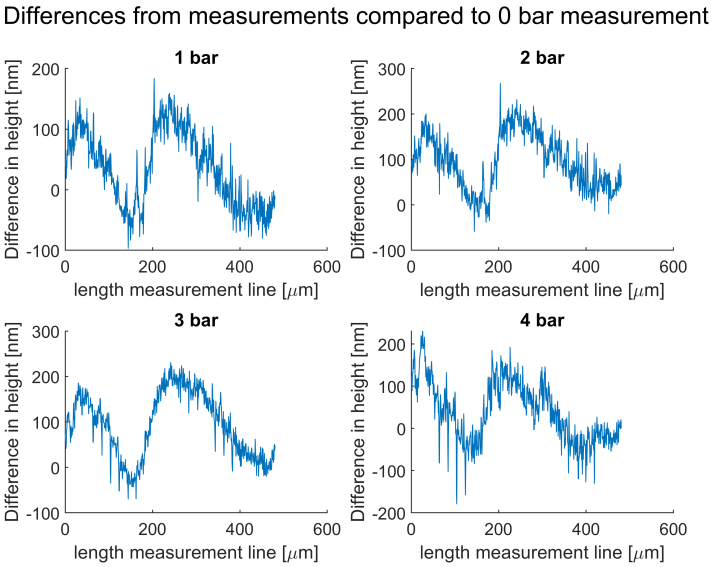

Figure 10: Differences in the height along the measurement with respect to the 0 bar measurement

Unfortunately, as can be seen, this does not give a very nice result. There are several things that seem to be going on. First, lets take a look at Figure 9. In the first 100 μm the material seems to behave normal and slightly rise. However, this also seems to happen in the 0 bar measurement which should not be the case. Next, around 150-200 μm the signal suddenly drops a few hundred nanometer.
When comparing these observations with the layout of the sensor there are two possible solutions. The first one is that around the 200 μm the material drops, this would mean that the roof would cave in a little because of the empty channel underneath. Another solution is that the microscope looks through the SiRN, which is transparent, and measures the bottom of the channel underneath. Both situations are not desirable and cannot easily be solved or avoided. Another observation is that there seem to be a lot of spikes and sudden differences in the measurement. Most likely, those spikes are caused by the etching holes that were created to make the channels. In between the etch holes still some original material is left, after fabrication the etching holes are filled with SiRN. The process of filling the etch holes can cause some deformations which do not lead to a flat surface.
Comparing the results of the four measurements visible in Figure 10 there are some differences distinguishable between the 1 bar and 2 bar measurement. However, the 3 and 4 bar measurements do not continue this rise.
Something else that became visible from the results is there was already a rise in height visible outside the sensor. Too investigate this some more post-measurement analysis was done. After averaging the substrate underneath the sensor the result in Figure 11 became visible. From the differences in colour underneath the sensor it becomes clear that the substrate is not flat. The red regions are higher as the blue regions. Because of this the sensor will also not be flat making it very hard to get a reliable result.

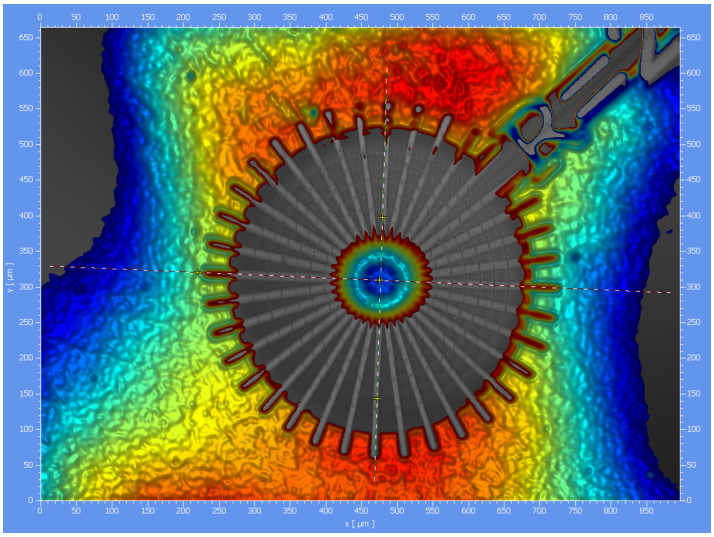

Figure 11: Picture from post-measurement analysis on one of the sensors under the vibrometer. Averaging shows that the substrate underneath the sensor is not a flat surface.

Due to the combination of the several observations it becomes clear that with the current measurement it is not possible to accurately determine the height of the sensor and from that calculate the elongation. Therefore, no further effort is put into this measurement and for the remainder of the research an estimated value of 210 GPa will be used as the Young's Modulus (E).

5.2 Resistances

The resistances of the sensors were measured on several chips using the method discussed in the previous chapter. The results from the two different wafers are visible in Table 3. There are several noticeable things about these results. The first thing that stands out is that the resistance values from Sensor 1-6 seem to differ a lot from the theoretic resistances. In theory the resistance should become higher as the sensor becomes longer, in reality the resistance does not rise as fast as expected. To investigate how this is possible a few representative chips are placed under a Single Electron Microscope (SEM). Using the SEM the exact dimensions of the resistors can be found. In Figure 12 a SEM picture is visible, this is a picture from pressure sensor 6 from a chip that comes from the 5194 wafer. Comparing this picture to the dimension from Figure 2b it is visible that the dimensions are different. The width of all the parts is roughly 1 μm more, this also decreases the length of the strain gauges. The bigger width and shorter length results in a lower resistance. As the length of the sensor increases this effect becomes bigger.

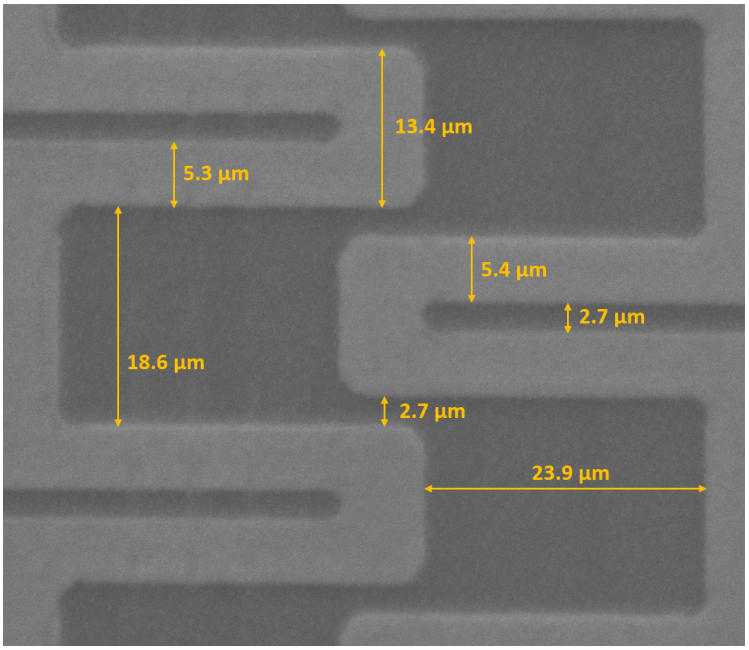

Figure 12: SEM picture of pressure sensor 6 on a chip from the 5194 wafer. All the dimensions are measured and displayed in µm.

Table 3: Results from resistance measurement. Resistances measured from Vcc to Ground.

Wafer 3046	Resistances of the sensors in Ohm [Ω]								
	Sensor 1	Sensor 2	Sensor 3	Sensor 4	Sensor 5	Sensor 6	Inlet	Outlet	Reference
chip 3.2	156	198.2	232.2	277.8	324	374.1	175.9	176.2	174.7
chip 4.8	154.8	197.8	232	278.7	328	378.2	177.2	176.3	175
chip 6.6	155	192.8	232.1	272.1	320	369.3	176.5	172.5	173.7
chip 8.3	154.5	196.5	230	275.3	322.5	370.8	175.8	172.8	175
chip 9.10	146.2	186	217.7	183.2	307.5	355.7	175.2	174.8	170.1
Average	**155.075**	**196.325**	**231.575**	**275.975**	**323.625**	**373.1**	**176.35**	**174.45**	**174.6**
Wafer 5194									
chip3.2	178.5	226.4	263.8	313.8	366.5	420	202.3	196.9	197.5
chip4.8	168.8	211.3	246.5	294	344.5	395.4	186.9	186.7	188
chip6.6	167.2	209.8	244.5	291.4	341.4	392.3	-	-	187.6
Average	**171.5**	**215.83**	**251.6**	**299.73**	**350.8**	**402.56**	**194.6**	**191.8**	**191.03**

Something else that is noticeable is highlighted in Table 3. The resistance value of sensor 4 on chip 9.10 is much lower compared to sensor 4 on other chips. After placing the chip under a microscope it seems that there is a small defect between two of the Wheatstone resistors, this defect most likely causes a short circuit. If this is indeed the case only half of the sensor would function, this would mean that the working part of sensor 4 is just as long as sensor 2. Looking at the measured values this is a viable result.

The last point is that there is a considerable difference in resistance between the two wafers. The difference seems to be quite consistent of roughly a 20 Ω difference between the two wafers. Due to the fabrication process there can be small resistance differences between wafers, however, a difference of 20 Ω is no longer in the range of a fer per cent. The chip numbers indicate their location on the wafer, chips of different wafers with the same number can be compared with each other to see if they behave the same. For both the wafers chips 3.2, 4.8 and 6.6 are compared with each other. Every sensor on those chips seems to roughly have the same deviation. The results are visible in Table 4. At this point there is no clear result that explains the difference in resistance between the two wafers. For the research it has no negative effect that the resistance differs, it is important to take the resistance difference into account when comparing results from different wafers.

Table 4: Identical chips from the two wafers are compared with each other. The resistance values per sensor of one chip are divided by the resistance value of the same sensor on the other chip.

chips	Sensor 1	Sensor 2	Sensor 3	Sensor 4	Sensor 5	Sensor 6	Inlet	Outlet	Reference
chip3.2	87.39 %	87.54 %	88.02 %	88.53 %	88.40 %	89.07 %	86.95 %	89.49 %	88.46 %
chip4.8	91.71 %	93.61 %	94.12 %	94.80 %	95.21 %	95.65 %	94.81 %	94.43 %	93.09 %
chip6.6	92.70 %	91.90 %	94.93 %	93.38 %	93.73 %	94.14 %	-	-	92.59 %

5.3 Dependence of length

All chips were measured to see if they responded as expected and too check if all the sensors worked. From this resulted that only one chip had 9 working sensors (chip 6.6 from wafer 5194), a second chip had 8 working sensors (chip 9.10 from wafer 3046). Both these chips are used in the coming sections to represent the results. The results of the first measurements are visible in Figures 13a & 13b. The legend for these figures is visible in Figure 14. Throughout the results the same colour scheme is used for the results, unless stated otherwise the legend applies for all the results. At every maximum the measurement is at 7 Bar, at every minimum the measurement is at 1.2 Bar. Note that this is the absolute pressure. From these figures it is not clear to see the difference between the sensors. Therefore, from these measurements two cycles are chosen to analyse more in-depth. These cycles are visible in Figures 15a & 15b.

There are some differences between the two chips that are easily spotted. First, chip 9.10 reaches a higher output for most of the sensors. In this chip all the functioning sensors are close to each other but they do give distinguishable results. The second thing is that around the starting point (five hours) it looks like something is interfering the sensors of chip 9.10. This does not occur at chip 6.6. Later on will be explained what most likely causes this disturbance. Something that stands out in the results of chip 6.6 is that the output gives a significant lower output compared to the input, which is interesting since both sensors have the same length. Also it is noticeable that all the sensors of chip 6.6 behave less linearly compared to chip 9.10. In Appendix C more results of measurements are visible. Those results show that there is a consistency between the sensors. At this point the usage of only two different chips is not good enough to say if the sensor can be considered consistent.

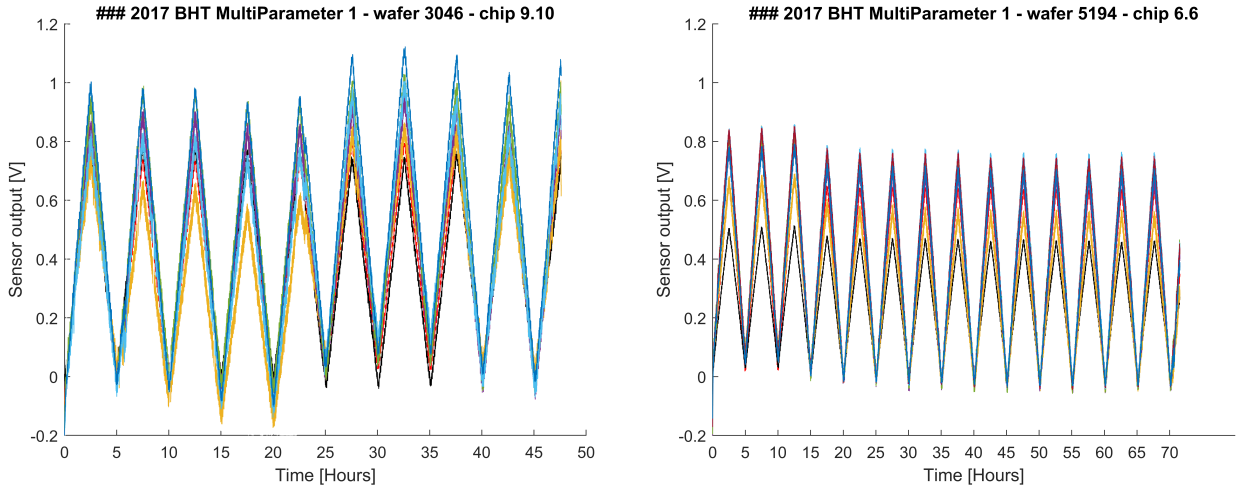

(a) *(b)*

Figure 13: (a) Total measurement from chip 9.10, the measurement performed 9 complete cycles. Note that sensor 5 is not displayed because it is defect. (b) Total measurement from chip 6.6, the measurement performed 14 complete cycles.

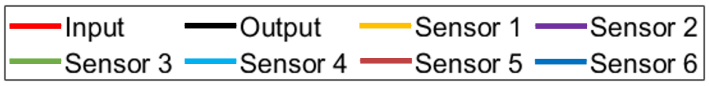

Figure 14: legend showing the colour scheme of the separate sensors. Used for multiple figures throughout the results.

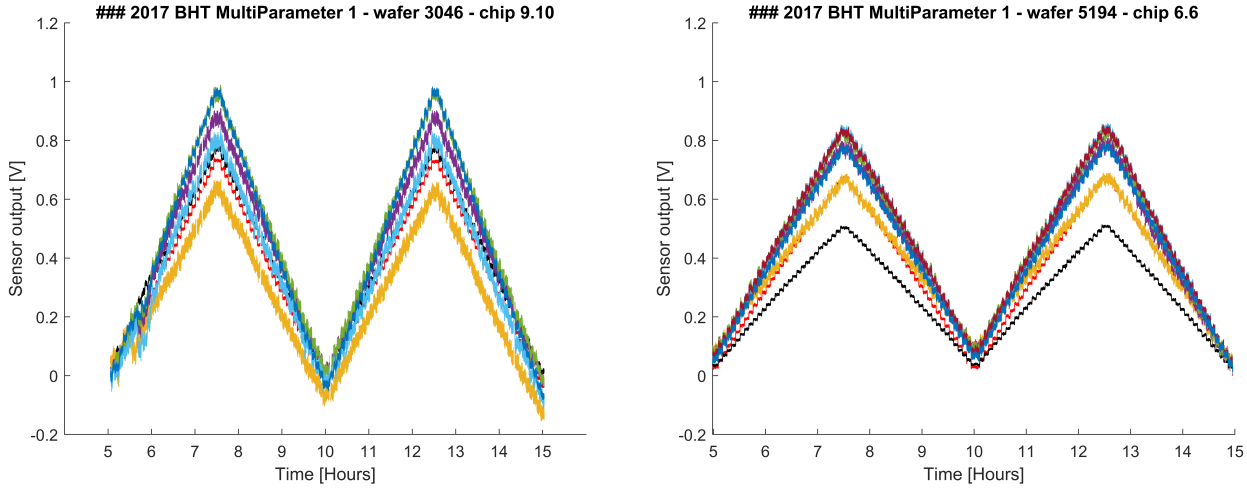

(a) *(b)*

Figure 15: (a) Sensor output versus the time of the the second and third cycle of chip 9.10. Note that sensor 5 is not displayed because it is defect. (b) Sensor output versus the time of the second and third cycle of chip 6.6.

5.4 Dependence temperature

Coming back to the weird behaviour of chip 9.10, around the fifth to sixth hour the sensors suddenly have a lot of interference. Since it is already the second measurement cycle this can not be explained as the start up phase. To find what causes this disturbance the measurement is compared with the temperature which is measured. Focusing on only the disturbance for this situation Figure 16 shows a zoomed in version of the time frame of the temperature. From this figure it is clear that around the same time frame there is a fluctuation in the temperature. Because the temperature is measured next to the measurement setup this is most likely caused by a change in room temperature (someone opening the door). It could also indicate that at that time someone touched or moved the measurement setup which causes the disturbance in the sensors.

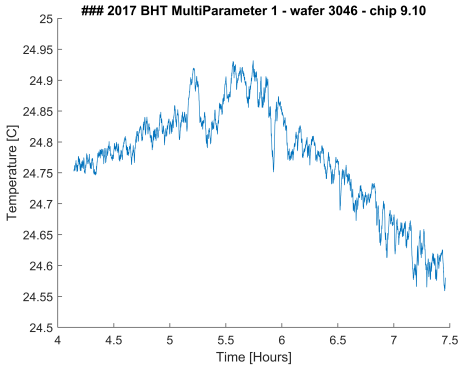

Figure 16: Temperature plotted versus time for chip 9.10. The focus is on the time frame of the disturbance, hours five to seven.

This relation between the disturbance and temperature gave some insight in the behaviour of the sensors. Looking back to Figures 13a & 13b it is visible that over time the peaks of the sensors change. Chip 9.10 gives a better view of this compared to chip 6.6 but it is visible in both. Too look at this dependence of temperature the sensors are compared with a reference sensor. The reference sensor is not subjected to a pressure so changes in sensitivity in this sensor would be weird. Normally the reference sensor is a flat line, which is why it is not visible in other results. In this case it is interesting to look at the reference sensor, the goal is to see if the reference sensor has the same response to temperature as the other sensors. In Figures 17a & 17b the reference sensor is plotted together with the temperature. Next to that, the average offset at every minimum point of the sensors is plotted. This offset is displayed with a margin which shows the standard deviation of each offset.

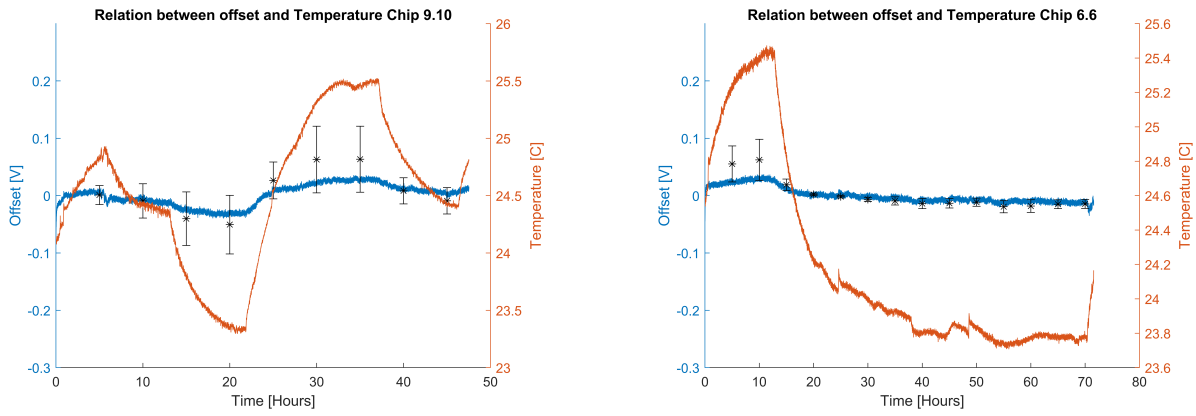

(a) *(b)*

Figure 17: (a) Temperature, offset and reference sensor plotted against time for chip 9.10. (b) Temperature, offset and reference plotted against time for chip 6.6. Similar behaviour is visible for all three signals

From Figures 17a & 17b it becomes clear that there certainly is a relation between the offset and temperature. Both the reference output and offsets of the sensors follow the behaviour of the temperature. In Figure 17b the offsets of the sensors are close to each other, where in Figure 17a they are more spread out. The results from these figures do indicate that the temperature has a influence on the offset. What is interesting to see is that at bigger deviations from the room temperature the offset has a larger deviation.

5.5 Relation noise and offset

To further look at the behaviour of the offset we take a step back. In the measurement setup each sensor is introduced with an offset, this is to balance the signal around 0.5 V so it will stay withing the range of the ADC. At the end of the process this introduced offset is subtracted from the output again. There are several things that can happen and go wrong in this process. If a measurement is started quickly without giving the sensor time to warm up there can already occur differences in the offset when it is initialised. Also, if the temperature influences the offset an incorrect number might be subtracted at the end. This could be one of the biggest contributors of noise in the output signals. To get a quantification on the size of the noise the standard deviation of each sensor is calculated. This standard deviation is compared to the introduced offset to see if there are any clear relations. The results of this for the chip 9.10 & 6.6 is visible in Figure 18. Visible from this figure is that there seems to be a pattern for most of the sensors. The input, output and reference sensors show a lower offset and standard deviation. For both chips sensor 1 is one of the sensors with the biggest offset and standard deviation.

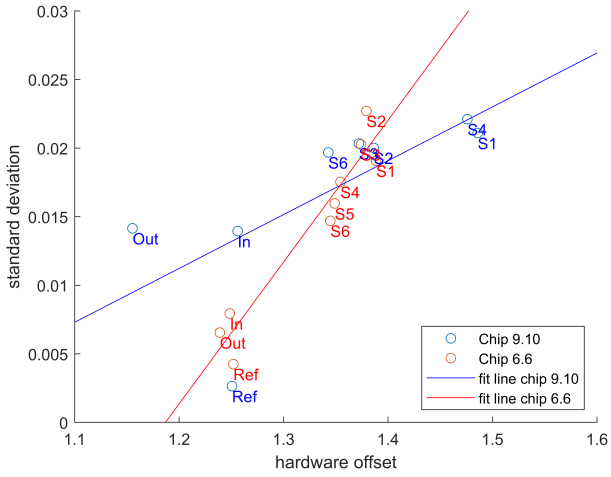

Figure 18: Standard deviation of the sensors plotted against the introduced offset. For chip 9.10 sensor five is not displayed because it is defect

To investigate interference from outside sources a measurement is done with a Faraday cage placed over the measurement setup. If there is interference from outside this should be visible when comparing the result with a normal measurement. For the measurement chip 9.10 is used. In Figure 19a the results from the two measurements from chip 9.10 are visible. Looking at this figure it is visible that both measurements with chip 9.10 have the same hardware offset. The standard deviation of the measurement with the Faraday case is lower. This is an indicator that there are indeed some interferences that are reduced by the Faraday cage. Looking at Figure 19b it can be seen that the standard deviation from the average offset is very low for this measurement. Comparing Figure 19b with Figure 17a it does stand out that the temperature behaves differently under the Faraday cage. The temperature for the measurement with the Faraday cage is higher, this can also have influence on the offset and make it more simple.

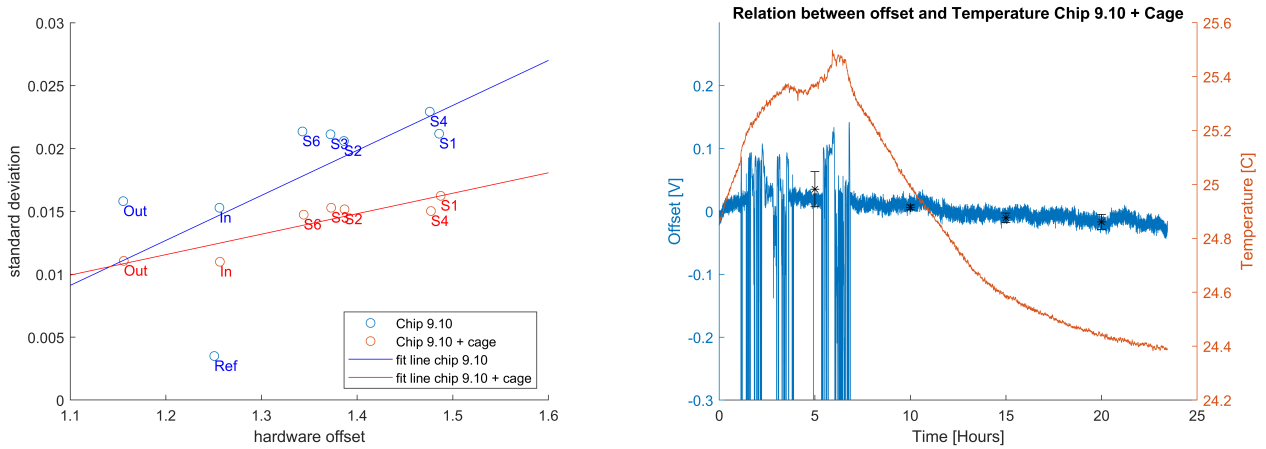

(a) *(b)*

Figure 19: (a) Standard deviation of the sensors plotted against the introduced offset. For chip 9.10 + cage the reference sensor is not displayed. (b) Temperature,offset and reference sensor plotted against time for chip 9.10 with a Faraday cage.

5.6 Comparison with theoretical model

Back in section 3.7 an expression was found for the theoretic sensor output. Now that there are results from the measurements those can be compared to the theory. As is explained in the theory the sensor output is slightly different for every sensor because of the difference in connecting wires for each sensor. For the pressure an equal range to the pressure used in the measurements is used. The theoretic sensor output is visible in Figure 20. From the measurements every cycle is averaged to get the sensor output. The results for chips 9.10 & 6.6 are visible in Figures 21a & 21b The legend visible in Figure 20 applies for both figures. Looking at the figures both chips show roughly the same results. The output of 9.10 is slightly better at higher pressures and acts more linear. Chip 6.6 becomes less linear at the higher pressures. For both the chips the sensitivity can be calculated from the output signals of the sensors. All the sensitivities are visible in Table 5.
Something which stands out immediately is that the theory has completely different values as the measurements. There are some factors that play a role in this difference. First of all the Young's Modulus has a linear relation with the sensor output. The estimated value that is used in the theoretical model can differ from the reality. The same applies for the input voltage and the amplification factor. It is already known that the dimensions of the strain gauges are not the same as in the theoretic model causing differences in the input voltage of the Wheatstone bridge. It is very likely that this deviation in the dimensions also occurs for the channel roof. In the equation for the strain (4) the length (L) and height (h) of the channel roof have a quadratic influence.

Table 5: Sensitivities from all the sensors of chips 9.10 & 6.6, and the theoretical sensitivities. All the sensitivities are in V/Bar.

	Sensitivities in V/Bar		
Sensor	Theory	Chip 9.10	Chip 6.6
Input	1.18	0.20	0.18
1	1.25	0.20	0.18
2	1.29	0.22	0.21
3	1.32	0.23	0.21
4	1.33	0.22	0.20
5	1.34	0.21	0.21
6	1.31	0.24	0.19
Output	1.31	0.19	0.14

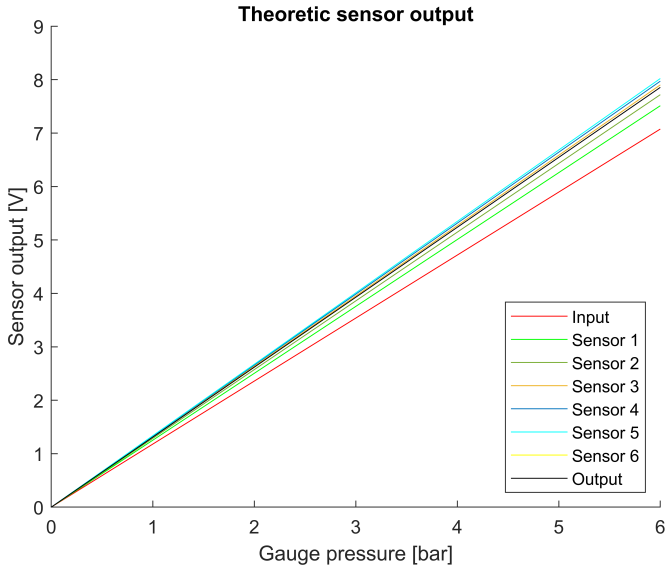

Figure 20: Sensor output based on the theoretical resistances and pressure. Results are presented in Gauge pressure.

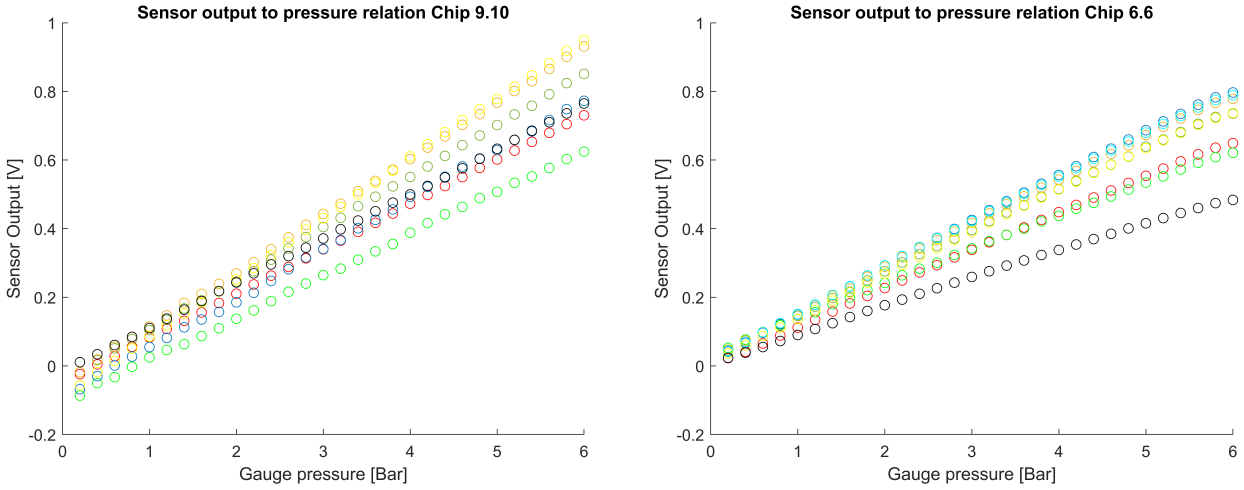

(a) *(b)*

Figure 21: (a) Sensor output of all channels of chip 9.10. Note that sensor 5 is not displayed because it is defect. (b) Sensor output of all channels of chip 6.6. Results are presented in Gauge pressure. Legend is visible in Figure 20.

6 Conclusion & Discussion

In this chapter the results are discussed further and reflected upon the four research questions set in chapter 4 and points of discussion will be explained in more detail.

Research question:
Can the elongation of the structure be measured accurately to determine the Young's Modulus of the material?

Based on the results from section 5.1 this research question can be answered easily. With the measurement method that was proposed it is not possible to accurately determine the Young's Modulus. There are several things that did not work as expected. First, from the results it looked as if the substrate around the channel and underneath the structures already had a curvature. This made it harder to find the elongation, because the curvature of the substrate should be subtracted from the results. A bigger problem is that the channels are relatively wide. They were created using three lines of etch holes next to each other, due to these etch holes the roof of the channel is never completely flat but shows a lot of small bumps on which the laser beam reflects. Also from the results it looked as if the middle of the structure slightly caved in. At 0 bar there was a drop in height of almost 400 nm. This makes analysing the behaviour of the roof more difficult because it has a different shape as expected. Another possibility is that the laser beam went through the SiRN layer and measured the bottom of the channel. This is a possibility because the SiRN is transparent. The combination of these factors gave very fluctuating and inconclusive results, as is visible in Figure 5.1. Because of the unreliable results it was better for the progress of the research to assume a value for the Young's Modulus. To improve this measurement preferably a different chip with smaller channels should be used and more attention should be paid to the actual shape of the channels to see if all the surfaces are flat before the measurements are performed.

Research question:
Are the measured resistances comparable to the theoretic resistances? If not, how can it be explained that the resistances are different from the theory?

Comparing Tables 2 & 3 it is clear that the measured resistances do not behave the same as the theoretic resistances. The explanation for this becomes clear when comparing Figure 2b with Figure 12. Due to the fabrication process the dimensions of the strain gauges are not exactly identical to the dimension in the theoretic model. There are small differences of around $1\mu m$. These differences occur for every single strain gauge, adding all the differences changes the value of the resistance significantly, especially for the longer sensors where there are more strain gauges. The difference is of less impact in the connecting wires, which causes differences in resistances for the different sensors. This explains why the resistance is lower compared to the theoretic resistances. The SEM pictures were taken after the deviation between theory and practice was discovered. Because of this the exact impact of the difference in size is unknown. This creates an uncertainty for the voltage that is entering the Wheatstone bridge, because it is unknown which percentage of the resistance is caused by the sensor and how much is caused by the connecting wires. With more time and measurements the exact percentage could be found to make the input voltage more accurate.

Research question:
Is there a distinguishable result between the output of the sensors? If so, can this result be explained by the contribution of the connecting wires?

Looking at Figures 13a & 13b there are definitely distinguishable results between the sensors. The same behaviour occurs in the theoretic model, which is visible in Figure 20. However, there are more differences that occur, looking at the sensitivities of the chips in Table 5 there is a considerable difference in the sensitivities of the chips and the theory. There are several contributing factors that play a role in this difference. First, the Young's Modulus. As is already discussed the Young's Modulus could not be accurately determined. Therefore a value is used that was obtained from previous research. However, the Young's modulus has a linear relation with the sensor output. Most likely the used value of the Young's modulus is lower then in reality.
Second, the input voltages are different then in theory because of the difference in resistance. Changing the input voltage has a direct impact on the sensor output. If the width of the connecting wires becomes bigger the resistance of those connecting wires becomes lower, resulting in a higher input voltage in the Wheatstone bridge.

Third, in the measurement there is a amplification factor of 38,649×. This value comes from the schematics of the AC readout modules. During the research this amplification was assumed to be correct. It is very likely that there is a deviation in this amplification, if the amplification factor is lower in reality the result of the theoretic model will seem too high. Another factor is the dimensions of the channel, in the equation for the strain (equation 4) the length (L), and height (h) of the channel roof have a quadratic relation. Because of the SEM pictures we already know that there is a deviation in the dimensions of the strain gauges. Most likely there are also deviations in the dimensions of the channel roof, this would cause differences in the sensor output. The combination of these factors can lead to a total deviation which is in the range of a factor 5. If the sensor of the output would be a factor 5 lower the results would become significantly closer to the reality. So, despite the current differences between the theoretic model and reality, it can be assumed that the results are reliable.

Research question:
Can the source of the noise be identified? If so, in what ways can the noise be minimised?

Analysis on the noise was mainly done in combination with the relation to temperature and offset. Looking back at the results of Figures 17a & 17b a clear relation can be seen between the temperature and the offset. Combining these results with Figure 18 it can be concluded that there is a relation between the offset and the standard deviation. The figure clearly shows that sensors which need to be compensated more also have a bigger deviation. The results from Figure 18 also are visible in Figures 15a & 15b, here the input and output sensors have an output that shows less noise compared to the other sensors. So, the temperature clearly has an influence on the size of the interference. But is it not the only source that causes interference. The measurement with the Faraday cage from Figure 19a shows a reduced standard deviation compared to the measurement without Faraday cage. This indicates that there is interference from the outside, which influences the deviation. However, at this point it is hard to prove this because only one measurement with a Faraday cage was done. The reduction in the standard deviation could also be caused by the accumalating heat in the Faraday cage, increasing the temperature.

Recommendations

Overall the sensors do seem to perform like expected from the theoretic model. But, at this point the sensor output seems to be largely dominated by the connecting wires. No irregularities are found in the results that indicate that the sensors behave differently if they become longer. There are some remarks to this that should be taken into account in future research. From the total amount of eight chips that were measured only two were performing good enough to do measurements with. Comparing two chips can already show some similarities or differences but to get reliable results more chips should be measured. If multiple chips still show the same similarities or differences it can be concluded that the results are reliable. Next to that it would be easier to look at the relevance of length if every sensor would have identical connecting wires. This would involve a more complicated chip design but would eliminate the uncertainties of the resistances and input voltages. Also, a better approximation of the Young's Modulus would lead to a more realistic theoretic model. The same holds for the measurement setup, if the exact amplitudes and amplification factors of the signals are known the model could be made better.

For reducing the noise a better temperature controlled environment would lead to less fluctuation in the offset and should reduce the deviation. If more information about the measurement setup is known, like the amplitudes and amplifications mentioned above, more could be known about noise that is added by the measurement setup. The results with the Faraday cage looked promising, this can definitely be investigated further by doing more measurements preferably with different chips. Also it would be beneficial to make a better Faraday cage in which the heat does not accumulate.

References

[1] D. Alveringh, T.V.P. Schut, R.J. Wiegerink, W. Sparreboom, and J.C. Lötters. Resistive pressure sensors integrated with a coriolis mass flow sensor, MESA+ Institute for Nanotechnology , University of Twente , Enschede , The Netherlands. (1):1167–1170, 2017.

[2] D. Alveringh, T. V.P. Schut, R.J. Wiegerink, W. Sparreboom, and J. C. Lötters. Micro Coriolis Mass Flowsensor With Integrated Resistive Pressure Sensors. *TRANSDUCERS 2017 - 19th International Conference on Solid-State Sensors, Actuators and Microsystems*, (October):1167–1170, 2017.

[3] M. Dijkstra, M.J. De Boer, J.W. Berenschot, T.S.J. Lammerink, R.J. Wiegerink, and M. Elwenspoek. Versatile Surface Channel Concept for Microfluidic Applications.

[4] Plasma-Therm. Silicon Nitride for MEMS Applications: LPCVD and PECVD Process Comparison. *MEMS and Sensors Whitepaper Series*, (January), 2014.

[5] R.J. Wiegerink, T.S.J. Lammerink, M. Dijkstra, and J. Haneveld. Thermal and Coriolis type micro flow sensors based on surface channel technology. *Procedia Chemistry*, 1(1):1455–1458, 2009.

[6] Warren C Young and Richard G Budynas. *Roark s Formulas for Stress and Strain*.

[7] J. Groenesteijn. *Microfluidic platform for Coriolis-based sensor and actuator systems*. 2016.

[8] T.V.P. Schut. Sensing of Multiple Parameters in a Micro-Fabricated Flow System, 2017.

[9] M.C. Elwenspoek, G.J.M Krijnen, R.J. Wiegerink, and T.S.J. Lammerink. *Introduction to Mechanics and transducer science*. University of Twente, Enschede, 2011.

[10] D. Alveringh, R.G.P. Sanders, J. Groenesteijn, and T.S.J. Lammerink. Universal modular fluidic and electronic interfacing platform for microfluidic devices, MESA+ Institute for Nanotechnology , University of Twente , Enschede , The Netherlands, Bronkhorst High-Tech BV , Ruurlo , The Netherlands. (October):4–6, 2017.

[11] T. V.P. Schut, D. Alveringh, W. Sparreboom, J. Groenesteijn, R. J. Wiegerink, and J. C. Lötters. Fully integrated mass flow, pressure, density and viscosity sensor for both liquids and gases. *Proceedings of the IEEE International Conference on Micro Electro Mechanical Systems (MEMS)*, 2018-Janua(January):218–221, 2018.

A Model theoretic resistances

3046

chip	sensor1	sensor2	sensor3	sensor4	sensor5	sensor6	inlet	outlet	ref	
chip4.8	154.8	197.8	232	278.7	328	378.2	177.2	176.3		175
chip3.2	156	198.2	232.2	277.8	324	374.1	175.9	176.2		174.7
chip6.6	155	192.8	232.1	272.1	320	369.3	176.5	172.5		173.7
chip8.3	154.5	196.5	230	275.3	322.5	370.8	175.8	172.8		175
chip 9.10	146.2	186	217.7	183.2	307.5	355.7				170.1
	153.3	**194.26**	**228.8**	**275.975**	**320.4**	**369.62**	**176.35**	**174.45**		**173.7**

length_conn_wires	3.00E-03	2.50E-03	2.00E-03	1.50E-03	1.00E-03	5.00E-04	1.17E-03	1.17E-03	1.51E-03
amount	30	46	60	76	92	108	46	46	46
length_output_arms	5.00E-04	7.50E-04	1.00E-03	1.25E-03	1.50E-03	1.75E-03			

5194

chip	sensor1	sensor2	sensor3	sensor4	sensor5	sensor6	inlet	outlet	ref	
chip3.2	178.5	226.4	263.8	313.8	366.5	420	202.3	196.9		197.5
chip4.8	168.8	211.3	246.5	294	344.5	395.4	186.9	186.7		188
chip6.6	167.2	209.8	244.5	291.4	341.4	392.3				187.6
Average	171.5	215.83333	251.6	299.73333	350.8	402.56667	194.6	191.8		191.0333333

connectors [length]			
S1	2.38E-03	2.04E-03	S6
S2	1.74E-03	1.46E-03	S5
S3	1.26E-03	1.16E-03	S4
input	9.60E-04	7.60E-04	
output	8.30E-04	9.00E-04	
reference	2.70E-04	7.00E-04	

	Sensor1	Sensor2	Sensor3	Sensor4	Sensor5	Sensor6			
R	179.75	220.66	253.75	297.65	347.40	399.59			
R_unadjusted	179.75486	259.60408	329.5514	407.73999	489.28885	570.8377	248.26	248.2597	250.0444534
	1	1.5	2	2.5	3	3.5			
		50%	33%	25%	20%	17%			
R_percentage	173	269.63229	345.27343	411.93925	489.28799	572.46795			
MATLAB	157.70637	241.81643	315.41273	399.52279	483.63286	567.74292			

Height_gauge	2.10E-07	area_gauge	8.61E-13			
Width_gauge	4.10E-06	area_conn	1.30E-12	A/L gauge	2.86E-10	
Width_conn	6.18E-06			A/L conn_sr	1.74E-09	
				A/L conn_lo	7.51E-10	
length_conn_small	1.24E-05			sum	2.78E-09	
length_conn_long	2.88E-05					
length_gauge	2.51E-05					
Width_wires	2.68E-05	area_wires	5.63E-12		1.88E-09	
width_output_arms	1.87E-05	area_arms	3.93E-12			
width_connectors	1.00E-04	area_connec	2.10E-11		4.41E-09	
				sum	9.07E-09	
area_bondpad	6.30E-11					
	0.0003					

									resistivity 2.92E-08
	sensor1	sensor2	sensor3	sensor4	sensor5	sensor6			
	1	0.85	0.77	0.73	0.71	0.7			
	sensor1	sensor2	sensor3	sensor4	sensor5	sensor6	input	output	reference
L/A	6.2E+09	8.9E+09	1.1E+10	1.4E+10	1.7E+10	2.0E+10	8.5E+09	8.5E+09	8.6E+09
	5.40E+09	8.28E+09	1.08E+10	1.37E+10	1.66E+10	1.95E+10	8.28E+09	8.28E+09	8.28E+09
R no connections	157.76818	241.9112	315.53635	399.67938	483.82241	567.96544	241.91	241.91	241.91
R connections	21.99	17.69	14.02	8.06	5.47	2.87	6.35	6.35	8.13
V_cc	0.13								
V_in	0.1140991	0.1211401	0.1244714	0.12743	0.1285476	0.1293459	0.12668	0.126676	0.125771462

B Measurement setup

In Table 6 the exact pin layout and connection with the baseboard is visible. The number under bondpad represents the bond pad number on the chip. Those numbers are visualised in Figure 22. The Pin number correspond to the pin connectors on the baseboard, which is visible in Figure 23. Under Sensor and Function is specified which pin connects to which sensor and what the function of that pin is.

Table 6: Pin layout and sensor functions of the big board and relation to the chipboard.

Bondpad	Pin	Sensor	Function
1	69	Pressure, inlet	V+
2	70	Pressure, inlet	Vcc
3	72	Pressure, inlet	V-
4	3		
5	4		
6	5	Pressure1	Vcc
7	13	Pressure1	V-
8	14	Pressure2	Vcc
9	15	Pressure2	V-
10	17	Pressure3	Vcc
11	18	Pressure3	V-
12	19	Pressure4	Vcc
13	20	Pressure4	V-
14	21	Pressure5	Vcc
15	23	Pressure5	V-
16	24	Pressure6	Vcc
17	25	Pressure6	V-
18	31		
19	32		
20	34	Pressure, outlet	Vcc
21	35	Pressure, outlet	V-
22	36	Pressure, outlet	GND
23	37	Pressure, outlet	V+
24	39	Pressure, ref	Vcc
25	40	Pressure, ref	V-
26	41	Pressure, ref	GND
27	42	Pressure, ref	V+
28	48	Pressure6	GND
29	49	Pressure6	V+
30	50	Pressure5	GND
31	52	Pressure5	V+
32	53	Pressure4	GND
33	54	Pressure4	V+
34	55	Pressure3	GND
35	56	Pressure3	V+
36	58	Pressure2	GND
37	59	Pressure2	V+
38	60	Pressure1	GND
39	62	Pressure1	V+
40	GND	Chip Ground	
41	GND	Chip Ground	
42			
43			
44	68	Pressure, inlet	GND

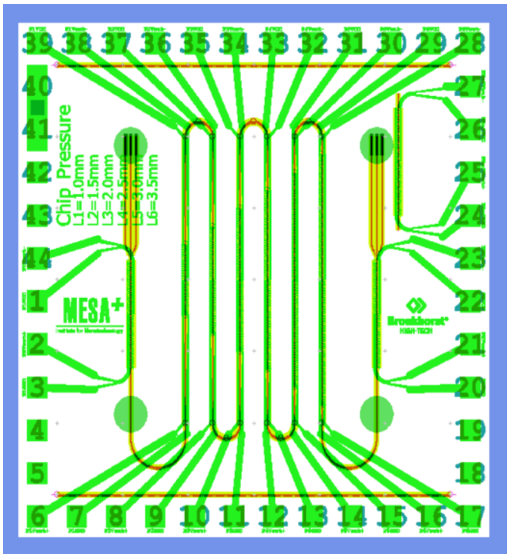

Figure 22: Chip design with all the bondpad numbered. Table 6 explains the function of each bondpad.

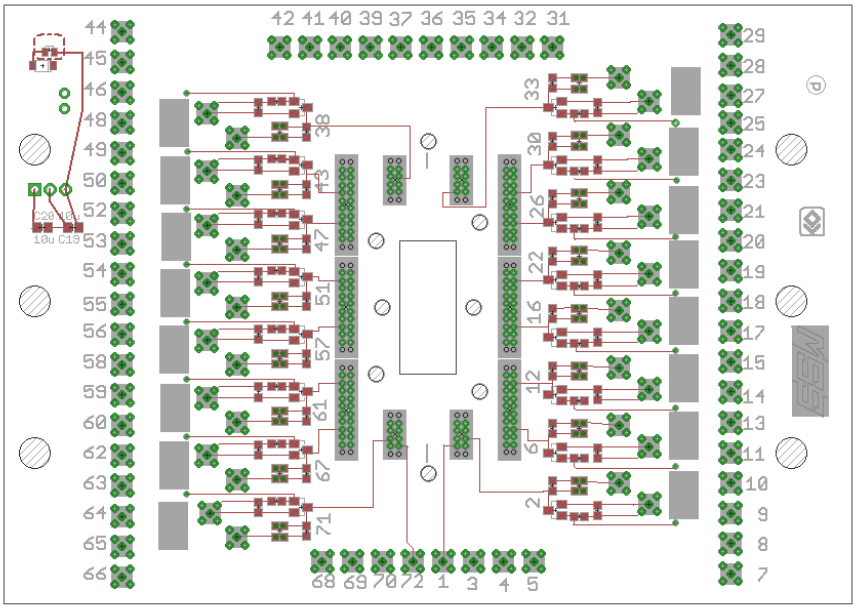

Figure 23: Layout of the baseboard. Numbers correspond with the Pin numbers in Table 6.

C Additional results

In this appendix additional results from measurements are presented. The results from these measurements are mostly repetition of measurements explained in chapter 4 but for different chips.

Results chip 9.10 with a Faraday cage

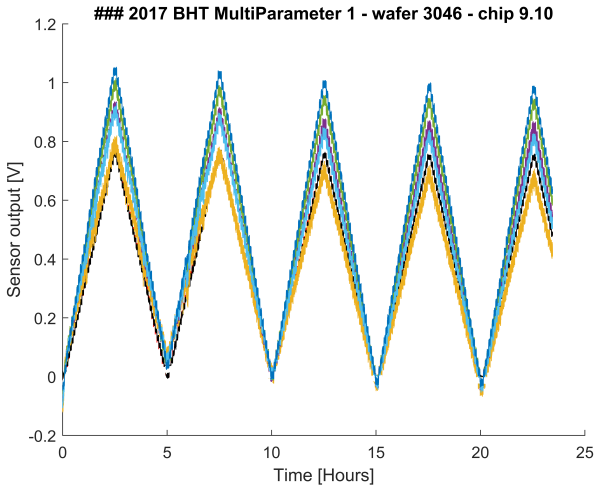

Figure 24: Total measurement from chip 9.10 with a Faraday cage. The measurement performed 4 complete cycles. Sensor 5 is not displayed because it is defect.

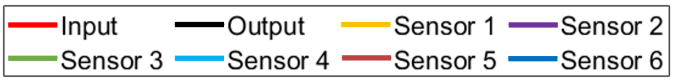

Figure 25: Legend showing the colour scheme used for the separate sensors.

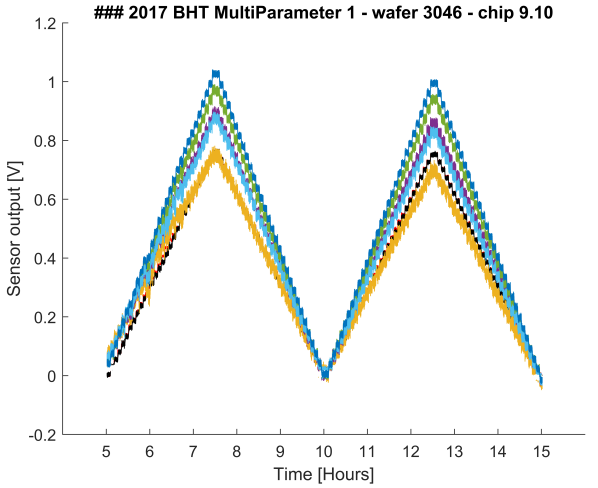

Figure 26: Sensor output versus the time of the second and third cycle. Sensor 5 is not displayed because it is defect.

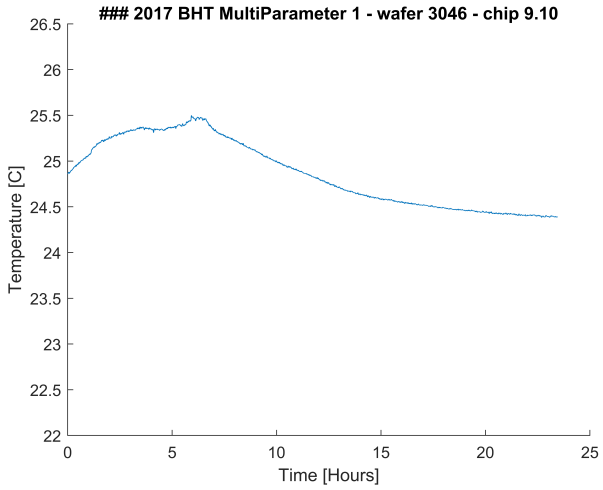

Figure 27: Temperature behaviour of chip 9.10 under a Faraday cage

Results separate sensor analysis

Too see if the different chips behaved in the same way the separate sensors are compared with each other. In the following figures sensor 1-6 are compared for three measurements. Chip 1 represents a normal measurement of chip 9.10. Chip 2 represents a measurement of chip 9.10 with a Faraday cage. Chip 3 represents a normal measurement of chip 6.6

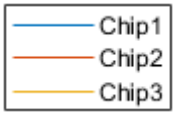

Figure 28: Legend used for the figures of the separate measurements

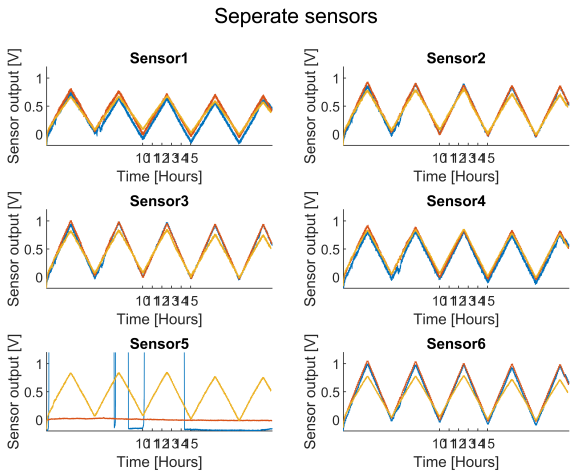

Figure 29: Results from comparing the sensors 1 to 6 with each other over multiple measurements

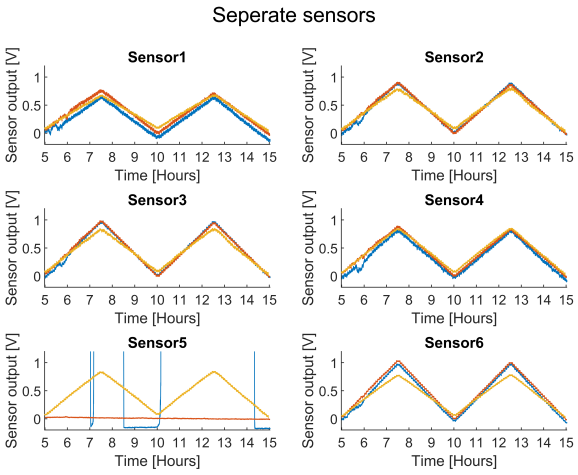

Figure 30: Results from comparing the sensors 1 to 6 with each other for the duration of two cycles.

D MATLAB code Theoretic model

In this appendix the MATLAB code used to create the theoretic model is displayed. The model uses a few text documents which include the dimensions, theoretic resistances and a few constants. The text documents are not included in the appendix.

```
dimension = importdata('C:\Users\Bas\OneDrive\Documenten\BO-IDS\Analytic_model_data\dimensions.txt');
sections = importdata('C:\Users\Bas\OneDrive\Documenten\BO-IDS\Analytic_model_data\integration_sections.txt');
constant = importdata('C:\Users\Bas\OneDrive\Documenten\BO-IDS\Analytic_model_data\constants.txt');
amount = importdata('C:\Users\Bas\OneDrive\Documenten\BO-IDS\Analytic_model_data\size_sensors.txt');
total_R = importdata('C:\Users\Bas\OneDrive\Documenten\BO-IDS\Analytic_model_data\theoretic_resistance.txt');
C = zeros(1,31);
strain = struct();
deflection = struct();
delta = struct();
Output = struct();
%% Creating Colors
color = struct();
color(11).data = [1 0 0]; %red
color(2).data = [0.8500 0.3250 0.0980];
color(3).data = [0 1 0]; %green
color(4).data = [0.4660 0.6740 0.1880];
color(12).data = [0 0 1]; %blue
color(6).data = [0 0.4470 0.7410];
color(7).data = [0 1 1]; %cyan
color(8).data = [0.3010 0.7450 0.9330];
color(9).data = [1 0 1]; %magenta
color(10).data = [0.6350 0.0780 0.1840];
color(1).data = [1 1 0]; %yellow
color(5).data = [0.9290 0.6940 0.1250];
color(13).data = [0 0 0]; %black
color(14).data = [1 1 1]; %white
%% Positions strain gauges in micrometer
stepsize = .1*10^-6;
length(1).length = sections.data(1,1):stepsize:sections.data(1,4);
length(2).length = sections.data(1,5):stepsize:sections.data(1,6);
length(3).length = sections.data(1,5):stepsize:sections.data(1,6);
length(4).length = sections.data(1,7):stepsize:sections.data(1,3);
length(5).zero = 0:stepsize:constant.data(1,1);
constant.bar = 0:.2:6;
%% Strain calculation
for j = 1:31
    for i =1:4
    C(j) = -(constant.bar(1,j).*10^5)./(2*constant.data(2,1)*dimension.data(1,7)^2);
      strain(i,j).strain = C(j).*(constant.data(1,1).^2-6.*length(i).length.*(constant.data(1,1)-length(i).length));
    end
end
```

```
strain0 = C(j).*(constant.data(1,1)^2-6*0:stepsize:constant.data(1,1)*(constant.data(1,1)-0:stepsize:constant.data(1,1)));
syms x
fun = (constant.data(1,1).^2.*x-6.*x.*constant.data(1,1)+6.*x.^2);
for j =1:31
    strain(1,j).average = double((1./dimension.data(1,1)).*C(j).*(int(fun,sections.data(1,1),sections.data(1,4))));
    strain(2,j).average = double((1./dimension.data(1,1))*C(j)*(int(fun,sections.data(1,5),sections.data(1,6))));
    strain(3,j).average = double((1./dimension.data(1,1))*C(j)*(int(fun,sections.data(1,5),sections.data(1,6))));
    strain(4,j).average = double((1./dimension.data(1,1))*C(j)*(int(fun,sections.data(1,7),sections.data(1,3))));
end
%% Deflection calculation
for k = 1:7
deflection(k).data = ((((k-1).*10^5)/(2*constant.data(2,1)*dimension.data(1,7)^3)).*length(5).zero.^2.*(constant.data(1,1)-length(5).zero).^2)*10^9;
end
%% Resistivity 1 resistor
constant.rho = (0.0476*constant.data(4,1)+0.9524*constant.data(3,1)); %average of the 2 materials
for k = 1:7
    Resistance.gauges(k) = constant.rho*((4*amount.data(k,1)*dimension.data(1,1))/(dimension.data(1,8)*dimension.data(1,6)));
    Resistance.connection(k) = constant.rho*((2*amount.data(k,1)*dimension.data(1,2))/(dimension.data(1,9)*dimension.data(1,6))+(2*amount.data(k,1)*dimension.data(1,3))/(dimension.data(1,9)*dimension.data(1,6)));
    Resistance.total(k) = Resistance.gauges(k) + Resistance.connection(k);
end
%% Wheatstone
%V_in = 0.45;
V_in = [0.394958334    0.419331014    0.430862553    0.44110395    0.444972503    0.447735747    0.438492667    0.438492667    0.435362754];
for j = 1:31
    for h = 1:9
        output(h).result(j) = V_in(h)*((1+2*constant.data(5,1))*(strain(2,j).average + strain(1,j).average)/2)*44595;
    end
end
%% Visual representation
n = 5;
figure(1)
hold on
cla
title('Strain over channel from 0 to 6 Bar (Gauge pressure)')
xlabel('channel width [\mum]')
ylabel('Relative elongation \Delta L/L')
for i=1:4
    name = ['strain',num2str(j)];
    for j = 1:n:31
        plot(length(i).length.*10^6,strain(i,j).strain)
    end
end
print(gcf,'strain','-dpng','-r600')
```

```
85 figure(2)
86 hold on
87 cla
88 title('Deformation over channel')
89 xlabel('channel width [\mum]')
90 ylabel('deflection [nm]')
91 for k = 1:7
92     plot(length(5).zero.*10^6,deflection(k).data)
93 end
94 legend('0 bar','1 bar','2 bar','3 bar','4 bar','5 bar','6 bar')
95 hold off
96 print(gcf,'deflection','-dpng','-r600')
97
98 P = struct();
99 figure(3)
100 hold on
101 cla
102 legend('Location','southeast')
103 title('Theoretic sensor output')
104 xlabel('Gauge pressure [bar]')
105 ylabel('Sensor output [V]')
106 plot(constant.bar,output(1).result,'color',color(11).data)
107 for h = 2:6
108     plot(constant.bar,output(h).result,'color',color(1+h).data)
109 end
110 plot(constant.bar,output(7).result,'color',color(1).data)
111 plot(constant.bar,output(8).result,'color',color(13).data)
112 legend('Input','Sensor 1','Sensor 2','Sensor 3','Sensor 4','Sensor 5','Sensor 6'
    ,'Output','Reference')
113 hold off
114 print(gcf,'sensor_output','-dpng','-r900')
115 for g = 1:8
116     P(g).slope = polyfit(constant.bar,output(g).result,1);
117     slope(g) = P(g).slope(1);
118 end
```

E MATLAB code Measurements

In this appendix the MATLAB code used to analyse all the measurement data is displayed.

```
1 input(1) = importdata('C:\Users\Bas\OneDrive\Documenten\BO-IDS\Measurements\
    Final\3046_9.10.dat');
2 input(2) = importdata('C:\Users\Bas\OneDrive\Documenten\BO-IDS\Measurements\
    Final\3046_9.10_kooi.dat');
3 input(3) = importdata('C:\Users\Bas\OneDrive\Documenten\BO-IDS\Measurements\
    Final\5194_6.6.dat');
4 chips = 3;
5 set = struct();
6 result = struct();
7 processed = struct();
8 for k = 1:chips
9     disp(input(k).textdata(2,1))
10    set(k).length = 1:length(input(k).data);
11    %set(k).length = 15000:27000;
```

```
12      %set(k).length = 1:84873;
13      %set(k).length = 1:169500;
14      set(k).setpoint = find(input(k).data(1:length(input(k).data),7) == 1.200);
15      %set(2).setpoint = find(input(2).data(1:300,7)==1.200);
16      for i = 1:9
17      result(i,k).average = mean(input(k).data(set(k).setpoint,i+8));
18      processed(i,k).data = input(k).data(set(k).length,8+i)-result(i,k).average;
19      end
20      for c = 1:8
21      processed(c,k).reference = processed(c,k).data-processed(9,k).data;
22      processed(c,k).diff = processed(c,k).data-processed(c,k).reference;
23      end
24 end
25 %S5 = 1.2414999999999998,
26 offset1 = [1.2559999999999993, 1.4856999999999945, 1.3861999999999965,
       1.372099999999997, 1.4758999999999947, 1.3427999999999976,
       1.1554000000000089, 1.2505999999999995];
27 offset2 = [1.2564999999999993, 1.4872999999999945, 1.3867999999999967,
       1.372799999999997, 1.4770999999999948, 1.3440999999999974,
       1.156000000000009];
28 offset3 = [1.2484999999999995, 1.3885999999999965, 1.3792999999999969,
       1.373999999999997, 1.3543999999999974, 1.3488999999999973,
       1.3446999999999976, 1.239, 1.2518999999999996];
29
30 disp('stage 1')
31 %% Creating Colors
32 color = struct();
33 color(11).data = [1 0 0]; %red
34 color(2).data = [0.8500 0.3250 0.0980];
35 color(3).data = [0 1 0]; %green
36 color(4).data = [0.4660 0.6740 0.1880];
37 color(12).data = [0 0 1]; %blue
38 color(6).data = [0 0.4470 0.7410];
39 color(7).data = [0 1 1]; %cyan
40 color(8).data = [0.3010 0.7450 0.9330];
41 color(9).data = [1 0 1]; %magenta
42 color(10).data = [0.6350 0.0780 0.1840];
43 color(1).data = [1 1 0]; %yellow
44 color(5).data = [0.9290 0.6940 0.1250];
45 color(13).data = [0 0 0]; %black
46 color(14).data = [1 1 1]; %white
47 disp('stage 2')
48  %% General measurement output change k for chip.
49 figure(1)
50 cla
51 hold on
52 legend
53 ylabel('Sensor output [V]');
54 xlabel('Time [Hours]');
55 for k = 1
56          legendi = 'Input';
57          legendo = 'Output';
58           title(input(k).textdata(2,1));
59           plot(input(k).data(set(k).length,1)./3600,processed(1,k).data,'
                 displayname',legendi,'color',color(11).data)
```

```
60            plot(input(k).data(set(k).length,1)./3600,processed(8,k).data,'
                  displayname',legendo,'color',color(13).data)
61      for i = 2:5
62            name = ['Sensor ',num2str(i-1)];
63            plot(input(k).data(set(k).length,1)./3600,processed(i,k).data,'
                  displayname',name)
64       %REMEMBER Sensor 5 is disabled because this is better for the display of
              chip 9.10
65      end
66          plot(input(k).data(set(k).length,1)./3600,processed(6,k).data,'
                displayname','Sensor 5','color',color(14).data)
67          plot(input(k).data(set(k).length,1)./3600,processed(7,k).data,'
                displayname','Sensor 6')
68          plot(input(k).data(set(k).length,1)./3600,processed(9,k).data,'
                displayname','Reference')
69 xlim([0 70])
70 ylim([-0.2 1.200001])
71 end
72 %print(gcf,'Chip1_output_1_cycle','-dpng','-r600')
73 %% noise analysis
74 wpass = 100;
75 for k = 1:chips
76 fs(k) =length(input(k).data);
77 end
78 xFit = linspace(1, 2, 50);
79 for c = 1:5
80     y1(c).data = highpass(processed(c,1).data,wpass,fs(1));
81     dev1(c) = std(y1(c).data(set(1).length,1));
82     y2(c).data = highpass(processed(c,2).data,wpass,fs(2));
83     dev2(c) = std(y2(c).data(set(2).length,1));
84 end
85 for c = 6:8
86     y1(c).data = highpass(processed(c+1,1).data,wpass,fs(1));
87     dev1(c) = std(y1(c).data(set(1).length,1));
88 end
89 for c = 6:7
90     y2(c).data = highpass(processed(c+1,2).data,wpass,fs(2));
91     dev2(c) = std(y2(c).data(set(2).length,1));
92 end
93 for c = 1:9
94     y3(c).data = highpass(processed(c,3).data,wpass,fs(3));
95     dev3(c) = std(y3(c).data(set(3).length,1));
96 end
97 poly1 = polyfit(offset1,dev1,1);
98 yFit1 = polyval(poly1,xFit);
99 poly2 = polyfit(offset2,dev2,1);
100 yFit2 = polyval(poly2,xFit);
101 poly3 = polyfit(offset3,dev3,1);
102 yFit3 = polyval(poly3,xFit);
103 figure(4)
104 cla
105 hold on
106 legend('Location','southeast')
107 xlim([1.1 1.6])
108 ylim([0 0.03])
```

```
109      plot(offset1,dev1,'o','displayname','Chip 9.10')
110      plot(offset2,dev2,'o','displayname','Chip 9.10 + cage')
111     % plot(offset3,dev3,'o','displayname','Chip 6.6')
112 plot(xFit,yFit1,'displayname','fit line chip 9.10','color',color(12).data)
113 plot(xFit,yFit2,'displayname','fit line chip 9.10 + cage','color',color(11).data
    )
114 %plot(xFit,yFit3,'displayname','fit line chip 6.6','color',color(11).data)
115 xlabel('hardware offset')
116 ylabel('standard deviation')
117 labels1 = {'In','S1','S2','S3','S4','S6','Out','Ref'};
118 labels2 = {'In','S1','S2','S3','S4','S6','Out'};
119 text(offset1,dev1,labels1,'color',color(12).data,'VerticalAlignment','top','
    HorizontalAlignment','left')
120 text(offset2,dev2,labels2,'color',color(11).data,'VerticalAlignment','top','
    HorizontalAlignment','left')
121 %text(offset3,dev3,labels2,'color',color(11).data,'VerticalAlignment','top','
    HorizontalAlignment','left')
122 print(gcf,'dev_offset_1and3','-dpng','-r600')
123 figure(2)
124 hold all
125 cla
126 for c = 2
127      plot(input(1).data(set(1).length,1)./3600,y1(c).data)
128 end
129 for c = 5
130      plot(input(1).data(set(1).length,1)./3600,y1(c).data)
131 end
132 disp('stage 3')
133 %% minima chip 1
134 amount = 10;
135 select = 1;
136 minima(1).length = 1:304;
137 minima(2).length =17834:18439;
138 minima(3).length =35971:36575;
139 minima(4).length =54071:54675;
140 minima(5).length =72169:72775;
141 minima(6).length =90187:90772;
142 minima(7).length =107852:108438;
143 minima(8).length =125484:126068;
144 minima(9).length =143107:143694;
145 minima(10).length =160738:161323;
146
147 half(1).length = 1:9382;
148 half(2).length = 18139:27504;
149 half(3).length = 35671:45036;
150 half(4).length = 53771:63136;
151 half(5).length = 71869:81234;
152 half(6).length = 89887:99252;
153 half(7).length = 107552:116917;
154 half(8).length = 125184:134549;
155 half(9).length = 142807:152172;
156 half(10).length = 160438:169803;
157 %% minima chip 2
158 amount = 5;
159 select = 2;
```

```
160 minima(1).length = 1:302;
161 minima(2).length = 17811:18413;
162 minima(3).length = 35982:36588;
163 minima(4).length = 54150:54752;
164 minima(5).length = 72287:72889;
165
166 half(1).length = 1      :      9366;
167 half(2).length = 17511  :      26876;
168 half(3).length = 35682  :      45047;
169 half(4).length = 53850  :      63215;
170 half(5).length = 7200   :      16565;
171 %% minima chip 3
172 amount = 15;
173 select = 3;
174 minima(1).length = 1:303;
175 minima(2).length = 17923:18529;
176 minima(3).length = 36146:36746;
177 minima(4).length = 54347:54956;
178 minima(5).length = 72545:73155;
179 minima(6).length = 90663:91260;
180 minima(7).length = 108460:109052;
181 minima(8).length = 126260:126852;
182 minima(9).length = 144029:144621;
183 minima(10).length = 161801:162392;
184 minima(11).length = 179548:180136;
185 minima(12).length = 197297:197889;
186 minima(13).length = 215021:215612;
187 minima(14).length = 232781:233372;
188 minima(15).length = 250503:251095;
189
190 half(1).length = 1      :      9366;
191 half(2).length = 17623  :      26988;
192 half(3).length = 35846  :      45211;
193 half(4).length = 54047  :      63412;
194 half(5).length = 72245  :      81610;
195 half(6).length = 90363  :      99728;
196 half(7).length = 108160 :      117525;
197 half(8).length = 12600  :      21965;
198 half(9).length = 143729 :      153094;
199 half(10).length = 161501      :      170866;
200 half(11).length = 179248     :      188613;
201 half(12).length = 197000     :      206365;
202 half(13).length = 2147021    :      2156386;
203 half(14).length = 232481     :      241846;
204 half(15).length = 250203     :      259568;
205 %% Test
206 steps = unique(input(1).data(half(5).length,7),'sorted');
207 for k = 1
208     for j = 1:length(steps)
209         for c = 1:8
210             for b = 1:amount
211                 B(b,j).data = find(input(1).data(half(b).length,7)==steps(j,1));
212                 B(b,j).average(c) = mean(input(1).data(B(j).data,8+c));
213             end
214         end
```

```
215     end
216 end
217
218  figure(11)
219  cla
220  hold all
221  title('Sensor output to pressure relation')
222  xlabel('Pressure [Bar]')
223 ylabel('Sensor Output [V]')
224 for j = 1:length(steps)
225     plot(steps(j,1),B(j,1).average(1),'-o','color',color(11).data)
226 end
227 P = polyfit(steps(j,1),B(j,1).average(1),1);
228 %Q = polyfit(steps(j,1),B(j,2).average(1),1);
229 %R = polyfit(steps(j,1),B(j,3).average(1),1);
230 %% Pressure output relation
231 A = struct();
232 steps = unique(input(k).data(set(k).length,7),'sorted');
233 for k = 1:chips
234     for j = 1:length(steps)
235         for c = 1:8
236             A(j,k).data = find(input(k).data(set(k).length,7)==steps(j,1));
237             A(j,k).average(c) = mean(input(k).data(A(j).data,8+c));
238         end
239     end
240 end
241 k =3;
242 figure(10)
243 cla
244 hold all
245 title('Sensor output to pressure relation Chip 6.6')
246 xlabel('Gauge pressure [Bar]')
247 ylabel('Sensor Output [V]')
248 ylim([-0.2 1])
249 for j = 1:length(steps)
250     plot(steps(j,1)-1,A(j,k).average(1)-result(1,k).average,'-o','color',color
        (11).data,'displayname','Input')
251     for c = 2:6
252         name = (['sensor',num2str(c-1)]);
253         plot(steps(j,1)-1,A(j,k).average(c)-result(c,k).average,'-o','color',
            color(1+c).data,'displayname',name)
254     end
255     plot(steps(j,1)-1,A(j,k).average(7)-result(7,k).average,'-o','color',color
        (1).data,'displayname','Sensor 6')
256     plot(steps(j,1)-1,A(j,k).average(8)-result(8,k).average,'-o','color',color
        (13).data,'displayname','Output')
257 end
258 print(gcf,'Chip3_sensor_output','-dpng','-r900')
259
260 for j = 1:length(steps)
261     for h = 1:8
262         P(h).slope1 = polyfit(steps(j,1),A(j,1).average(h),1);
263         slope1(h) = P(h).slope1(1);
264         P(h).slope2 = polyfit(steps(j,1),A(j,3).average(h),1);
265         slope2(h) = P(h).slope2(1);
```

```
266     end
267 end
268 Sensitivity_chip1 = mean(slope1)
269 Sensitivity_chip3 = mean(slope2)
270 %% offset/temperature
271 for k = select
272 for b = 1:amount
273     for j = 1:5
274 minima(b).average(j) = mean(processed(j,k).data(minima(b).length,1));
275 average(b) = mean(minima(b).average);
276 dev(b) = std(minima(b).average);
277     end
278         for j = 7:8
279 minima(b).average(j) = mean(processed(j,k).data(minima(b).length,1));
280 average(b) = mean(minima(b).average);
281 dev(b) = std(minima(b).average);
282     end
283 %temp = normalize(input(k).data(set(k).length,8))*.1;
284 temp = input(k).data(set(k).length,8);
285 end
286 figure(3)
287 cla
288 hold on
289 title('Relation between offset and Temperature Chip 9.10 + Cage')
290 xlabel('Time [Hours]')
291 ylabel('Offset [V]')
292 ylim([-.3 .3])
293 yyaxis right
294 ylabel('Temperature [C]')
295 p2 =plot(input(k).data(set(k).length,1)./3600,temp)
296 yyaxis left
297 p1 =plot(input(k).data(set(k).length,1)./3600,processed(9,k).data)
298 for b = 1:amount-1
299         errorbar(b.*5,average(b+1),dev(b+1),'-*','color',color(13).data)
300 end
301 print(gcf,'offset_temperature_chip2','-dpng','-r900')
302 end
303 %% All chips
304 figure(8)
305 cla
306 hold on
307 ylabel('Sensor output [V]');
308 xlabel('Time [Hours]');
309 for k = 1:chips
310     title('Combination of chips');
311     legendi = ['Pinput chip', num2str(k)];
312     legendo = ['Poutput chip', num2str(k)];
313     plot(input(k).data(set(k).length,1)./3600,processed(1,k).data,'displayname',
        legendi,'color',color(11).data)
314     plot(input(k).data(set(k).length,1)./3600,processed(8,k).data,'displayname',
        legendo,'color',color(13).data)
315     for i = 2:7
316          name = ['Chip', num2str(k),'Sensor',num2str(i-1)];
317          plot(input(k).data(set(k).length,1)./3600,processed(i,k).data,'
             displayname',name);%,'color',color(i-1).data);
```

```
318     end
319 end
320 xticks(0:1:50)
321 ylim([-0.2 1.200001])
322 print(gcf,'Chips_all','-dpng','-r900')
323 %% Seperate measurements
324 figure(9)
325 sgtitle('Seperate sensors');
326 for i = 1:6
327 subplot(3,2,i);
328 cla
329 %legend
330 hold on
331 ylabel('Sensor output [V]');
332 xlabel('Time [Hours]');
333 title(['Sensor',num2str(i)]);
334 %for k = 1:chips
335 %name1 = ['Chip',num2str(k)];
336 plot(input(1).data(set(1).length,1)./3600,processed(i+1,1).data,'displayname','
    wafer3046 chip9.10')
337 plot(input(2).data(set(2).length,1)./3600,processed(i+1,2).data,'displayname','
    wafer3046 chip9.10 + faraday cage')
338 plot(input(3).data(set(3).length,1)./3600,processed(i+1,3).data,'displayname','
    wafer5194 chip6.6')
339 %end
340 end
341 print(gcf,'seperate sensors','-dpng','-r900')
342 disp('end')
```